[4] S. Murase, E. Mosser, E.M. Schuman, Depolarization drives beta-catenin into neuronal spines promoting changes in synaptic structure and function, Neuron 35 (2002) 91–105.
[5] A.C. Hall, F.R. Lucas, P.C. Salinas, Axonal remodeling and synaptic differentiation in the cerebellum is regulated by WNT-7a signaling, Cell 100 (2000) 525–535.
[6] M. Kitagawa, S. Hatakeyama, M. Shirane, M. Matsumoto, N. Ishida, K. Hattori, I. Nakamichi, A. Kikuchi, K. Nakayama, An F-box protein, FWD1, mediates ubiquitin-dependent proteolysis of beta-catenin, EMBO J. 18 (1999) 2401–2410.
[7] J. Behrens, J.P. von Kries, M. Kuhl, L. Bruhn, D. Wedlich, R. Grosschedl, W. Birchmeier, Functional interaction of beta-catenin with the transcription factor LEF-1, Nature 382 (1996) 638–642.
[8] O. Tetsu, F. McCormick, Beta-catenin regulates expression of cyclin D1 in colon carcinoma cells, Nature 398 (1999) 422–426.
[9] X. Yu, R.C. Malenka, Beta-catenin is critical for dendritic morphogenesis, Nat. Neurosci. 6 (2003) 1169–1177.
[10] S.X. Bamji, K. Shimazu, N. Kimes, J. Huelsken, W. Birchmeier, B. Lu, L.F. Reichardt, Role of beta-catenin in synaptic vesicle localization and presynaptic assembly, Neuron 40 (2003) 719–731.
[11] B. De Strooper, P. Saftig, K. Craessaerts, H. Vanderstichele, G. Guhde, W. Annaert, K. Von Figura, F. Van Leuven, Deficiency of presenilin-1 inhibits the normal cleavage of amyloid precursor protein, Nature 391 (1998) 387–390.
[12] P. Marambaud, J. Shioi, G. Serban, A. Georgakopoulos, S. Sarner, V. Nagy, L. Baki, P. Wen, S. Efthimiopoulos, Z. Shao, T. Wisniewski, N.K. Robakis, A presenilin-1/gamma-secretase cleavage releases the E-cadherin intracellular domain and regulates disassembly of adherens junctions, EMBO J. 21 (2002) 1948–1956.
[13] Y. Gu, H. Misonou, T. Sato, N. Dohmae, K. Takio, Y. Ihara, Distinct intramembrane cleavage of the beta-amyloid precursor protein family resembling gamma-secretase-like cleavage of Notch, J. Biol. Chem. 276 (2001) 35235–35238.
[14] E.H. Schroeter, J.A. Kisslinger, R. Kopan, Notch-1 signalling requires ligand-induced proteolytic release of intracellular domain, Nature 393 (1998) 382–386.
[15] I. Okamoto, Y. Kawano, D. Murakami, T. Sasayama, N. Araki, T. Miki, A.J. Wong, H. Saya, Proteolytic release of CD44 intracellular domain and its role in the CD44 signaling pathway, J. Cell Biol. 155 (2001) 755–762.
[16] E.H. Koo, R. Kopan, Potential role of presenilin-regulated signaling pathways in sporadic neurodegeneration, Nat. Med. 10 (Suppl.) (2004) S26–S33.
[17] M.S. Wolfe, R. Kopan, Intramembrane proteolysis: theme and variations, Science 305 (2004) 1119–1123.
[18] A. Georgakopoulos, P. Marambaud, S. Efthimiopoulos, J. Shioi, W. Cui, H.C. Li, M. Schutte, R. Gordon, G.R. Holstein, G. Martinelli, P. Mehta, V.L. Friedrich Jr., N.K. Robakis, Presenilin-1 forms complexes with the cadherin/catenin cell–cell adhesion system and is recruited to intercellular and synaptic contacts, Mol. Cell. 4 (1999) 893–902.
[19] P. Marambaud, P.H. Wen, A. Dutt, J. Shioi, A. Takashima, R. Siman, N.K. Robakis, A CBP binding transcriptional repressor produced by the PS1/epsilon-cleavage of N-cadherin is inhibited by PS1 FAD mutations, Cell 114 (2003) 635–645.
[20] R.D. Terry, E. Masliah, D.P. Salmon, N. Butters, R. DeTeresa, R. Hill, L.A. Hansen, R. Katzman, Physical basis of cognitive alterations in Alzheimer's disease: synapse loss is the major correlate of cognitive impairment, Ann. Neurol. 30 (1991) 572–580.
[21] K. Uemura, N. Kitagawa, R. Kohno, A. Kuzuya, T. Kageyama, H. Shibasaki, S. Shimohama, Presenilin 1 mediates retinoic acid-induced differentiation of SH-SY5Y cells through facilitation of Wnt signaling, J. Neurosci. Res. 73 (2003) 166–175.
[22] K. Uemura, N. Kitagawa, R. Kohno, A. Kuzuya, T. Kageyama, K. Chonabayashi, H. Shibasaki, S. Shimohama, Presenilin 1 is involved in maturation and trafficking of N-cadherin to the plasma membrane, J. Neurosci. Res. 74 (2003) 184–191.
[23] A. Kinoshita, C.M. Whelan, C.J. Smith, I. Mikhailenko, G.W. Rebeck, D.K. Strickland, B.T. Hyman, Demonstration by fluorescence resonance energy transfer of two sites of interaction between the low-density lipoprotein receptor-related protein and the amyloid precursor protein: role of the intracellular adapter protein Fe65, J. Neurosci. 21 (2001) 8354–8361.
[24] K. Reiss, T. Maretzky, A. Ludwig, T. Tousseyn, B. de Strooper, D. Hartmann, P. Saftig, ADAM10 cleavage of N-cadherin and regulation of cell–cell adhesion and beta-catenin nuclear signalling, EMBO J. 24 (2005) 1762.
[25] K. Uemura, T. Kihara, A. Kuzuya, K. Okawa, T. Nishimoto, H. Bito, H. Ninomiya, H. Sugimoto, A. Kinoshita, S. Shimohama, Characterization of sequential N-cadherin cleavage by ADAM10 and PS1, *Neurosci Lett. (in press)*.
[26] M.S. Wolfe, W. Xia, B.L. Ostaszewski, T.S. Diehl, W.T. Kimberly, D.J. Selkoe, Two transmembrane aspartates in presenilin-1 required for presenilin endoproteolysis and gamma-secretase activity, Nature 398 (1999) 513–517.
[27] P.H. Wen, P.R. Hof, X. Chen, K. Gluck, G. Austin, S.G. Younkin, L.H. Younkin, R. DeGasperi, M.A. Gama Sosa, N.K. Robakis, V. Haroutunian, G.A. Elder, The presenilin-1 familial Alzheimer disease mutant P117L impairs neurogenesis in the hippocampus of adult mice, Exp. Neurol. 188 (2004) 224–237.
[28] I.G. Haas, M. Frank, N. Veron, R. Kemler, Presenilin-dependent processing and nuclear function of gamma-protocadherins, J. Biol. Chem. 280 (2005) 9313–9319.
[29] J.J. Otero, W. Fu, L. Kan, A.E. Cuadra, J.A. Kessler, Beta-catenin signaling is required for neural differentiation of embryonic stem cells, Development 131 (2004) 3545–3557.
[30] W.J. Nelson, R. Nusse, Convergence of Wnt, beta-catenin, and cadherin pathways, Science 303 (2004) 1483–1487.
[31] A. Chenn, C.A. Walsh, Regulation of cerebral cortical size by control of cell cycle exit in neural precursors, Science 297 (2002) 365–369.
[32] C.A. Saura, S.Y. Choi, V. Beglopoulos, S. Malkani, D. Zhang, B.S. Shankaranarayana Rao, S. Chattarji, R.J. Kelleher, E.R. Kandel, K. Duff, A. Kirkwood, J. Shen, Loss of presenilin function causes impairments of memory and synaptic plasticity followed by age-dependent neurodegeneration, Neuron 42 (2004) 23–36.
[33] B. Dermaut, S. Kumar-Singh, S. Engelborghs, J. Theuns, R. Rademakers, J. Saerens, B.A. Pickut, K. Peeters, M. van den Broeck, K. Vennekens, S. Claes, M. Cruts, P. Cras, J.J. Martin, C. Van Broeckhoven, P.P. De Deyn, A novel presenilin 1 mutation associated with Pick's disease but not beta-amyloid plaques, Ann. Neurol. 55 (2004) 617–626.
[34] D.J. Selkoe, Alzheimer's disease is a synaptic failure, Science 298 (2002) 789–791.

Available online at www.sciencedirect.com
ScienceDirect
Neuroscience Research 56 (2006) 459–469
Neuroscience Research
www.elsevier.com/locate/neures

Developmental expression of neural Wiskott–Aldrich syndrome protein (N-WASP) and WASP family verprolin-homologous protein (WAVE)-related proteins in postnatal rat cerebral cortex and hippocampus

Daiju Tsuchiya [a], Yoshihisa Kitamura [a], Kazuyuki Takata [a], Tatsuhiko Sugisaki [a], Takashi Taniguchi [a], Kengo Uemura [b,c], Hiroaki Miki [d], Tadaomi Takenawa [d], Shun Shimohama [b,*]

[a] *Department of Neurobiology, 21st Century COE Program, Kyoto Pharmaceutical University, Kyoto 607-8414, Japan*
[b] *Department of Neurology, Graduate School of Medicine, Kyoto University, 54 Shogoin-Kawahara-cho, Sakyo-ku, Kyoto 606-8507, Japan*
[c] *Horizontal Medical Research Organization, Graduate School of Medicine, Kyoto University, Kyoto 606-8507, Japan*
[d] *Division of Biochemistry, Institute of Medical Science, University of Tokyo, Tokyo 108-8639, Japan*

Received 10 July 2006; accepted 7 September 2006
Available online 16 October 2006

Abstract

The actin cytoskeleton plays a critical role in the cellular morphological changes. Its organization is essential for neurite extension and synaptogenesis under the processes of neuronal development. Recently, neural Wiskott–Aldrich syndrome protein (N-WASP) and WASP family verprolin-homologous protein (WAVE) have been identified as key molecules, which specifically participate in regulation of actin cytoskeleton through small GTPases. The functions of these factors have been investigated using cultured cells; however, *in vivo* developmental changes in these factors are not fully understood. In this study, we examined the expression levels and distributions of N-WASP, WAVE and their related proteins in the rat cerebral cortex and hippocampus during postnatal development. Protein levels of these factors were progressively increased during development, and actin was accumulated in membranous fractions. Immunoreactivities for these factors were widely but differentially observed in entire brain. In the developing brain, N-WASP and WAVE seemed to exist in the synapse-rich areas, such as stratum radiatum of hippocampal CA1 subfield. A similar tendency in the distributions of these factors was observed in the mature brain. Taken together, N-WASP, WAVE and their related proteins may participate in normal brain development and synaptic plasticity by regulating the actin cytoskeleton.

Keywords: N-WASP; WAVE; Actin cytoskeleton; Postnatal rat brain; Protein level; Distribution; Development

1. Introduction

The nervous system is a highly organized network of cellular interactions formed by neurons. Its function depends on the complex architecture of neuronal networks, and this complexity arises from the staggering morphological intricacy of neurons. Sprouting and elongation of axons and dendrites, at the right time and in the right direction, form the basis of proper neuronal connectivity and, consequently, brain function (Shepherd, 2004). This neuroanatomical morphogenesis is driven by the dynamics of intracellular cytoskeletons, such as actin filaments and microtubules (Da Silva and Dotti, 2002).

The actin cytoskeleton plays a critical role in the regulation of cellular morphological change in response to various extracellular stimuli. In addition, its organization is essential for cell migration, neurite extension and synaptogenesis in the processes of neuronal maturation and development (Luo, 2002; Whitford et al., 2002). In the early steps of neuronal development, actin filaments have been shown to accumulate at growth cone, a guidance apparatus located at the tip of growing neurites (Dickson, 2002; Dent and Gertler, 2003). It has long been suggested that actin cytoskeletal reorganization at growth cones, including filopodium and lamellipodium formation, is the key determinant of the direction and/or speed

* Corresponding author. Present address: Department of Neurology, Sapporo Medical University School of Medicine, S1W17, Chuo-ku, Sapporo 060-8556, Japan. Tel.: +81 11 622 2111x3820; fax: +81 11 622 7668.
E-mail address: shimoha@sapmed.ac.jp (S. Shimohama).

0168-0102/$ – see front matter
doi:10.1016/j.neures.2006.09.007

of neurite extension (Da Silva and Dotti, 2002). Thus, clarification of the regulatory mechanism behind the reorganization of the actin cytoskeleton in neurons will ultimately lead to better understanding of neuronal development.

Evidences have been accumulated about regulatory mechanisms in dynamics of the actin filaments. This signaling cascade is governed by small GTPases of the Ras-homologous member (Rho) family. Among them, RhoA, Rac and Cdc42 play critical roles in the formation and organization of actin networks. In particular, Cdc42 and Rac have been shown to induce the filopodia and lamellipodia thought to be the basis for inducing the synapse formation (Threadgill et al., 1997; Bishop and Hall, 2000). Recently, neural Wiskott–Aldrich syndrome protein (N-WASP) (Miki et al., 1996) and WASP family verprolin-homologous protein (WAVE) (Miki et al., 1998b) have been identified as key molecules, which specifically participate in the formation of filopodium and lamellipodium through Cdc42 and Rac, respectively (Fig. 1; Takenawa and Miki, 2001; Da Silva and Dotti, 2002). *In vitro* reconstitution studies revealed that N-WASP is activated via Cdc42 in the presence of phosphatidylinositol 4,5-bisphosphate (PIP_2), and then induces actin polymerization through the complex of actin-related protein 2/3 (Arp2/3) (Miki et al., 1998a). In addition, N-WASP-induced filopodium formation was facilitated by WASP interacting SH3 protein (WISH) in a Cdc42-independent manner (Fukuoka et al., 2001). On the other hand, WAVE-induced actin polymerization for lamellipodium formation was mediated by Rac1 and other factors through the dissociation of inhibitory complexes (Miki et al., 2000; Eden et al., 2002). Thus, these molecules are the key regulatory factors for neuronal morphogenesis and function. However, developmental changes in these molecules that regulate actin assembly are not fully understood. In the present study, we examined the expression levels and distributions of N-WASP and WAVE, and their related proteins in the rat cerebral cortex and hippocampus during postnatal development.

2. Materials and methods

2.1. Animals and materials

Wistar rats (Japan SLC, Inc., Hamamatsu, Japan) were used. The animals were acclimated to and maintained at 23 °C on a 12/12 h light/dark cycle (lights on 08:00–20:00 h). All animals were housed in standard laboratory cages and had free access to food and water throughout the study period. All animal experiments were carried out in accordance with the National Institutes of Health Guide for the Care and Use of Laboratory Animals, and the protocols were approved by the Committee for Animal Research at Kyoto Pharmaceutical University.

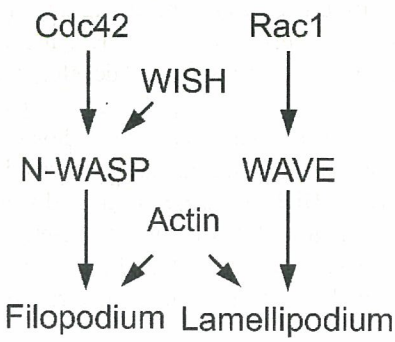

Fig. 1. Regulatory factors for actin cytoskeleton and the putative signaling pathway.

Antibodies against N-WASP or WISH were prepared as previously described (Miki et al., 1998a; Fukuoka et al., 2001). Other primary antibodies included rabbit polyclonal antibodies to actin (Sigma, St. Louis, MO, USA), WAVE (Santa Cruz Biotechnology, Santa Cruz, CA, USA); and mouse monoclonal antibodies to Cdc42 (Santa Cruz Biotechnology), Rac1 (BD Transduction Laboratories, San Jose, CA, USA), MAP2 (Clone HM-2, Sigma), GAP43 (clone GAP7B10, Sigma), synaptophysin (clone SY38, Dako, Glostrup, Denmark) and *N*-methyl-D-aspartate receptor-1 (NMDAR1, Chemicon International, Temecula, CA, USA) were used.

The ABC Elite kit from Vector Laboratories (Burlingame, CA, USA), enhanced chemiluminescent detection system kit (ECL kit) from Amersham Pharmacia Biotech (Buckinghamshire, UK), and the Bradford protein assay from BioRad Laboratories (Hercules, CA, USA) were used.

2.2. Immunoblotting and semi-quantitative analysis

Cerebral cortices and hippocampi were dissected from the brains of Wistar rats (age: 0, 3 and 7 days; 2, 3, 4 and 16 weeks) under deep anesthesia. The tissues were homogenized in 50 mM Tris–HCl buffer (pH 7.4) containing 1 mM EGTA, 1 mM EDTA, 1 mM phenylmethysulfonyl fluoride (PMSF) and 1 μg/ml leupeptin. The homogenate was centrifuged at 50,000 × *g* at 4 °C for 20 min, and the resulting supernatant was used as the cytosolic fraction. The pellet was resuspended with same buffer, washed three times by centrifugation, and then used as the membrane fraction. Protein concentration was determined using the Bradford protein assay kit according to the manufacturer's protocol.

Aliquots containing 10 μg of protein were analyzed by sodium dodecyl sulfate (SDS)-polyacrylamide gel electrophoresis (SDS-PAGE) and then transferred to polyvinylidene difluoride (PVDF) membrane (Immobilon-P, Millipore, Bedford, MA, USA). Immunoblotting was performed by transferring the proteins to a sheet of PVDF membrane by electroelution at a constant voltage of 100 V for 90 min at 4 °C. The PVDF membrane was incubated with Tris-buffered saline (pH 8.0) containing 0.05% Tween 20 (TBS-T) and 5% dehydrated skimmed milk (Difco Laboratories, Detroit, MI, USA) to block non-specific protein binding. The membrane was then incubated with an antibody to N-WASP (diluted 1:1000), WISH (1:5000), WAVE (1:1000), Cdc42 (1:100), Rac1 (1:1000) or actin (diluted 1:1000) followed by the secondary antibody, horseradish peroxidase (HRP)-linked antibodies against either rabbit or mouse immunoglobulin (each diluted 1:1000). Subsequently, bound HRP-labeled antibodies were detected by chemiluminescence (ECL kit). The protein bands that reacted with the antibodies were detected on radiographic film (X-Omat JB-1; Kodak, Rochester, NY) 5–60 s after exposure.

For semi-quantitative analysis, the bands of these proteins on radiographic films were scanned with a CCD color scanner (DuoScan, AGFA, Leverkusen, Germany) and then analyzed. Densitometric analysis was performed using the public domain NIH Image 1.56 program (written by Wayne Rasband at the U.S. National Institutes of Health and available from the Internet by anonymous ftp from http://zippy.nimh.nih.gov.).

Results regarding the densitometric analysis of immunoblots are given as the mean ± standard error of the mean (S.E.M.). The statistical significance of differences was determined by analysis of variance (ANOVA). Further statistical analysis for *post hoc* comparisons was carried out using the Bonferroni/Dunn test.

2.3. Immunohistochemistry

The brains were fixed in a cold fixative consisting of 4% paraformaldehyde in 100 mM phosphate buffer (PB) at 4 °C for 3 days. The brain was then transferred to 15% sucrose solution in 100 mM PB containing 0.1% sodium azide at 4 °C. Sections, 20-μm thick, were cut on a cryostat and collected in 100 mM PBS containing 0.3% Triton-X 100 (PBS-T). After several washes, the sections were stored until use in a free-floating state at 4 °C. The free-floating sections were incubated with the primary antibody against N-WASP (diluted:

1:800), WISH (1:800), WAVE (1:100), Cdc42 (1:50), Rac1 (1:50), actin (1:500), GAP43 (1:5000), synaptophysin (1:1000) or NMDAR1 (1:50) for 4 days at 4 °C. The sections were incubated with rat normal serum-adsorbed biotinylated anti-mouse or anti-rabbit IgG antibody (1:2000) for 2 h at room temperature and then incubated with avidin-biotinylated peroxide (ABC Elite kit, Vector Laboratories) for 1 h at room temperature. After each incubation, all sections were washed several times with PBS-T. Labeling was revealed by incubation with 50 mM Tris–HCl buffer, pH 7.6, containing 0.02% 3,3′-diaminobenzidine (DAB), 0.0045% hydrogen peroxide and 0.6% nickel ammonium sulfate. After several minutes, sections washed with PBS-T were mounted on a glass slide and coverslipped. The immunostained sections were scanned using a high resolution CCD digital camera ProgRes 3008 (Carl Zeiss, Jena, Germany).

For double immunolabeling, sections were incubated with primary antibodies against WISH (1:400) and GAP43 (1:3000). The primary antibodies were detected by Alexa 488-labeled anti-rabbit IgG antibody and Alexa 546-labeled anti-mouse IgG antibody (each diluted 1:500, Molecular Probes, Eugene, OR, USA), and the fluorescence was then observed using a laser scanning confocal microscope LSM410 (Carl Zeiss).

2.4. Neuronal culture and immunocytochemistry

Cerebral cortices were dissected from postnatal 0-day-old Wistar rats, and then minced. Tissue suspension was dispersed by 0.25% trypsin/EDTA and 0.01% DNase I, and resuspended in serum-free Dulbecco's modified Eagle medium (DMEM) including 2% B-27 supplement (Invitrogen, Carlsbad, CA, USA) and antibiotics. Cells were plated onto glass-coverslips coated with polyethyreneimine (Sigma), and incubated at 34 °C in 5% CO_2. To abolish the growth of non-neuronal cells, 2 μg/ml of aphidicolin (Sigma) was added into cultures on day *in vitro* (DIV) 2–6. The cultured neurons could be maintained for at least 2 months *in vitro* (data not shown). Neurons on DIV 5–7 were used in this study.

For immunocytochemical analysis, cells were fixed with 4% paraformaldehyde for 30 min at 4 °C. Cells were incubated for 4 days at 4 °C with primary antibodies against N-WASP (1:500), WISH (1:1000) or WAVE (1:200) in PBS containing 0.05% Triton-X 100. The cells were simultaneously incubated with anti-MAP2 antibody (1:3000). The primary antibodies were detected by appropriate secondary antibodies linked to Alexa 488 or Alexa 350 (each diluted 1:500, Molecular Probes). Rhodamine-conjugated phalloidin (1:40, Molecular Probes) was used to visualize actin filaments (F-actin). The fluorescence was observed using LSM410.

3. Results

3.1. Developmental changes in protein expression of actin and its regulators in rat brain

Fig. 1 shows the signaling cascade of actin cytoskeleton regulatory factors. Briefly, N-WASP and WAVE facilitate the formation of filopodium or lamellipodium through activation by Cdc42 and Rac1, respectively (Takenawa and Miki, 2001). WISH also activates N-WASP in a Cdc42-indepent manner. Therefore, we assessed the protein levels of these factors in developing rat brains by immunoblot analysis (Figs. 2 and 3). We prepared both cortical and hippocampal homogenates separated into cytosolic and membranous fractions, and then samples were subjected to SDS-PAGE and immunodetection. The levels of N-WASP and WISH in both fractions of the cerebral cortex and hippocampus were markedly increased in a development-dependent manner (Fig. 2A and B). WAVE protein levels were up-regulated in both fractions of the cortex and hippocampus in a development-dependent manner, and peaked in the 4-week-old brain (Fig. 2C). Cdc42 and Rac1 were

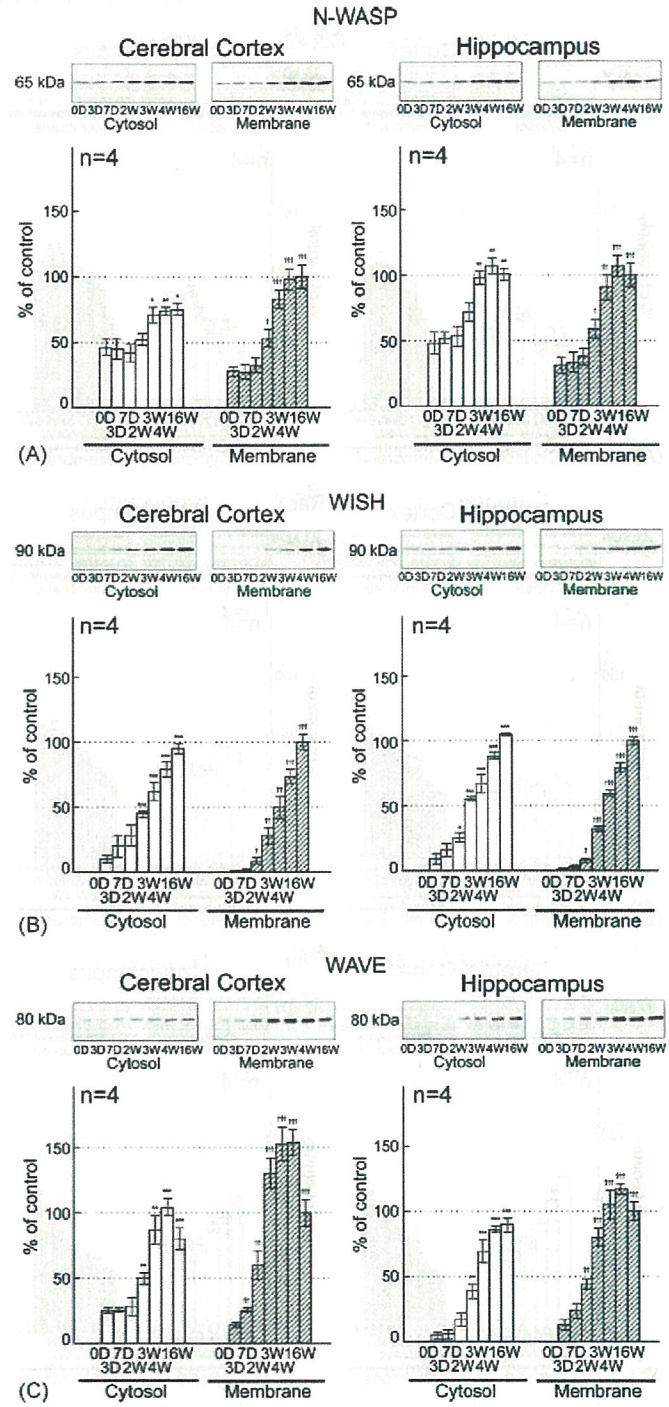

Fig. 2. Developmental changes in protein expression of N-WASP, WISH and WAVE in the rat cerebral cortex and hippocampus. The cytosolic and membranous fractions of cerebral cortices and hippocampi (age: 0 and 3 days, 1, 2, 3, 4 and 16 weeks) were subjected to immunoblot analysis (upper panels) of antibodies against N-WASP (A), WISH (B) and WAVE (C), and then the protein bands of 65-kDa N-WASP, 90-kDa WISH and 80-kDa WAVE were assessed (lower panels). The density of the protein band in the membranous fraction of 16-week-old rats was taken as 100%. Each value is the mean ± S.E.M. of four rats. $^{*}P < 0.05$, $^{**}P < 0.01$, $^{***}P < 0.001$ vs. the cytosolic fraction of 0-day-old rats. $^{\dagger}P < 0.05$, $^{\dagger\dagger}P < 0.01$, $^{\dagger\dagger\dagger}P < 0.001$ vs. the membranous fraction of 0-day-old rats.

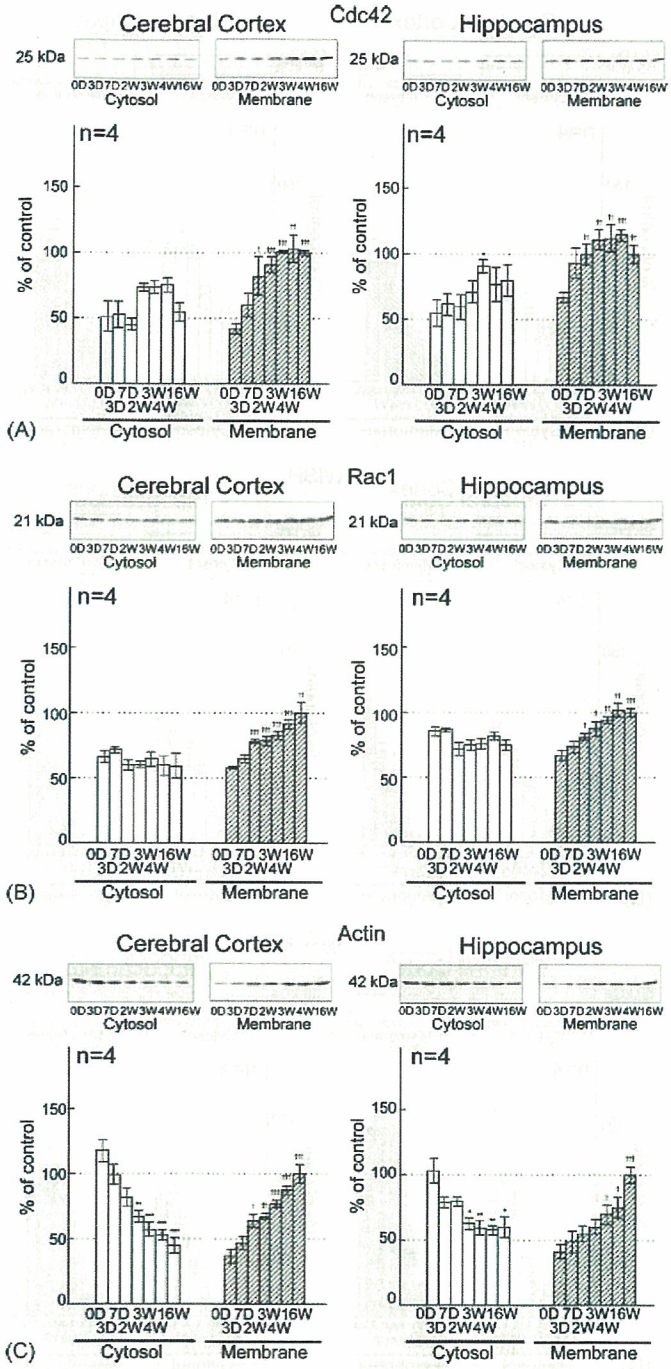

Fig. 3. Developmental changes in protein levels of Cdc42, Rac1 and actin in the rat cerebral cortex and hippocampus. The cytosolic and membranous fractions of cerebral cortices and hippocampi were prepared from rats, aged 0 and 3 days, 1, 2, 3, 4 and 16 weeks. Each sample was subjected to immunoblot analysis (upper panels) of antibodies against Cdc42 (A), Rac1 (B) and actin (C), and then the protein band of 25-kDa Cdc42, 21-kDa Rac1 and 42-kDa actin was assessed (lower panel). The density of the protein band in the membranous fraction of 16-week-old rats was taken as 100%. Each value is the mean ± S.E.M. of four rats. $^{*}P < 0.05$, $^{**}P < 0.01$, $^{***}P < 0.001$ vs. the cytosolic fraction of 0-day-old rats. $^{\dagger}P < 0.05$, $^{\dagger\dagger}P < 0.01$, $^{\dagger\dagger\dagger}P < 0.001$ vs. the membranous fraction of 0-day-old rats.

significantly increased in membranous fractions of both the cortex and hippocampus in a development-dependent manner, but were not markedly changed in the cytosolic fractions (Fig. 3A and B). Protein levels of actin were significantly increased in the membranous fractions of cerebral cortex in a development-dependent manner, although those in the cytosolic fractions were significantly decreased (Fig. 3C). Similar changes in the levels in the hippocampus were also observed (Fig. 3C).

3.2. Distribution of N-WASP, WAVE and their related factors in 2-week-old rat brain

Next, we immunohistochemically elucidated the localization of actin-related factors. In the brain of 2-week-old rat, when dendritic spines and synapses have begun to form and mature (Harris et al., 1992; Boyer et al., 1998), immature laminar structures of cortex and hippocampus were observed (Fig. 4).

In the cerebral cortex, immunoreactivities of N-WASP, WISH and WAVE were moderately observed throughout cortical layers as well as those of Cdc42 and Rac1 (Fig. 4A–E). An abundant distribution of actin was ubiquitously and homogenously observed throughout the cortex and hippocampus (Fig. 4F). Moderate expressions of GAP43, synaptophysin, which are presynaptic proteins, and NMDAR1, a postsynaptic receptor, were also detected in the entire cortex (Fig. 4G–I).

In hippocampal formation, distributions of N-WASP, WISH and WAVE were inhomogeneous throughout the laminar structures of CA1-3 subfields and the dentate gyrus (DG) (Fig. 4A–C). Expression patterns of Cdc42 and Rac1, as well as those of GAP43 and synaptophysin, also appeared inhomogeneous (Fig. 4D, E, G and H). In contrast, NMDAR1 immunoreactivity (Fig. 4I) showed negative and positive staining when comparing the distributions of GAP43 and synaptophysin (Fig. 4G and H).

3.3. Distribution of N-WASP, WAVE and their related factors in 16-week-old rat brain

In the brain of 16-week-old rat, the cortex and hippocampus in particular were enlarged, and laminar structures of both the cerebral cortex and hippocampal formation were obviously developed (Fig. 5). In the cortex, N-WASP immunoreactivity was observed moderately within the parenchyma, and punctate dense immunoreactivity was also detected (Fig. 5A). WISH and Cdc42 were expressed moderately in the neuropilar region; intensively in the neurites of neurons, such as cortical pyramidal cells, and weakly in the corpus callosum (Fig. 5B and D). Immunoreactivities of WAVE and Rac1 were observed throughout the cortex (Fig. 5C and E). The widespread immunoreactivity of actin was shown intensively in almost the entire brain, but only moderately in the corpus callosum and stratum alveus of the hippocampus (Fig. 5F). GAP43 immunoreactivity was distributed in neuropil and neurites (Fig. 5G), whereas synaptophysin was expressed in the neuropilar area, but was negatively expressed in the corpus callosum (Fig. 5H).

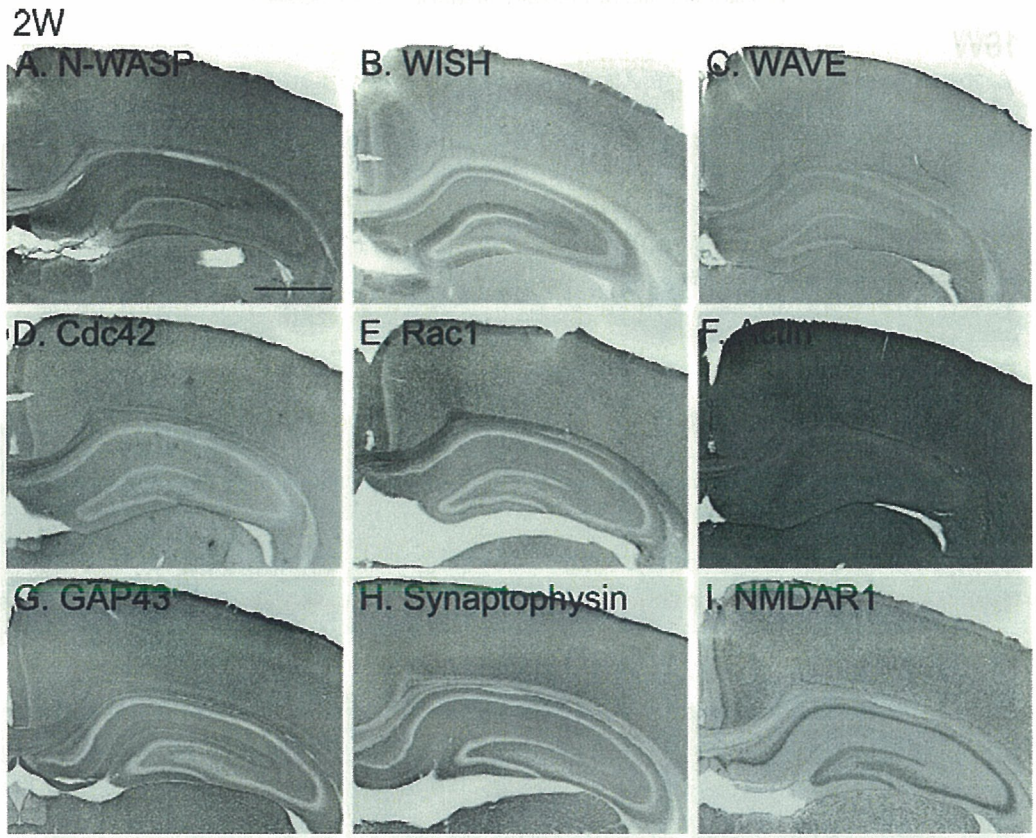

Fig. 4. Immunohistochemical localization of neuronal proteins in developing brains of 2-week-old rats. Immunoreactivities for N-WASP (A), WISH (B), WAVE (C), Cdc42 (D), Rac1 (E), actin (F), GAP43 (G), synaptophysin (H) and NMDAR1 (I) are shown in each panel. Scale bar = 1 mm.

In contrast, higher immunoreactivity of NMDAR1 was mainly restricted to the neuronal perikarya (Fig. 5I).

In hippocampal formation, N-WASP immunoreactivity was observed intensively in the pyramidal cells of CA1 and CA2, and moderately throughout other regions of the hippocampus (Fig. 5A). Expressions of WISH, WAVE, Cdc42 and Rac1 appeared as inhomogeneous patterns in laminar structures of the hippocampus, as well as the expression patterns of GAP43 and synaptophysin (Fig. 5B–E, G and H). In contrast, a higher expression of NMDAR1 was predominantly seen in the neuronal cell bodies of CA1–3 and DG areas, and this pattern had a negative–positive relation to other proteins (Fig. 5I).

3.4. Laminar distribution patterns of neuronal proteins in the CA1 and hilus of DG of hippocampal formation

Furthermore, we compared the immunoreactive patterns of neuronal proteins in hippocampal laminar structures of the CA1 region and hilus of DG at high magnification (Fig. 6). In the 2-week-old brain (Fig. 6, upper panels), Cdc42, WISH and N-WASP immunoreactivities were observed moderately throughout the hippocampus, *i.e.*, strata oriens, radiatum and lacunosum-moleculare of the CA1 and the molecular layer and hilus of DG (Fig. 6A–C). The stratum pyramidale of CA1 and the granule cell layer of DG showed sparse immunolabeling of Cdc42 and WISH, although N-WASP was expressed in the perikarya of pyramidal and granule cell layers. Thus, Cdc42, WISH and N-WASP immunoreactivities were relatively similar, but identical. In addition, higher immunoreactivity of Cdc42 was detected in the inner molecular layer of DG, whereas that of WISH was detected in the outer and middle molecular layers, suggesting that the expressing areas are different between Cdc42 and WISH, although these proteins are N-WASP activators. Immunoreactivities of Rac1 and WAVE were detected weakly in the stratum pyramidale of CA1 and the granule cell layer of DG; intensively in the inner molecular layer of DG, and moderately in other regions of the hippocampus (Fig. 6D and E). Diffuse immunoreactivity of MAP2, a dendritic marker *in vivo*, was observed throughout the hippocampus except stratum alveus of CA1 and neuronal perikarya of stratum pyramidale and granule cell layer (Fig. 6F). Strong immunoreactivity of MAP2 was also detected radially in the stratum radiatum of CA1. MAP2 was little in the stratum alveus of CA1. GAP43 and synaptophysin were distributed throughout the hippocampus, but the stratum pyramidale of CA1 and the granule cell layer of DG did not show immunoreactivities of GAP43 and synaptophysin (Fig. 6G and H). In contrast, strong NMDAR1 immunoreactivity was restricted to the neuronal perikarya of the stratum pyramidale of CA1 and the granule cell layer and hilus of DG (Fig. 6I). Thus, Cdc42, WISH, N-WASP, Rac1 and WAVE appeared to exist in the GAP43- or synaptophysin-immunoreactive regions, but NMDAR1 immunoreactivity was relatively opposite to immunoreactivities of other proteins.

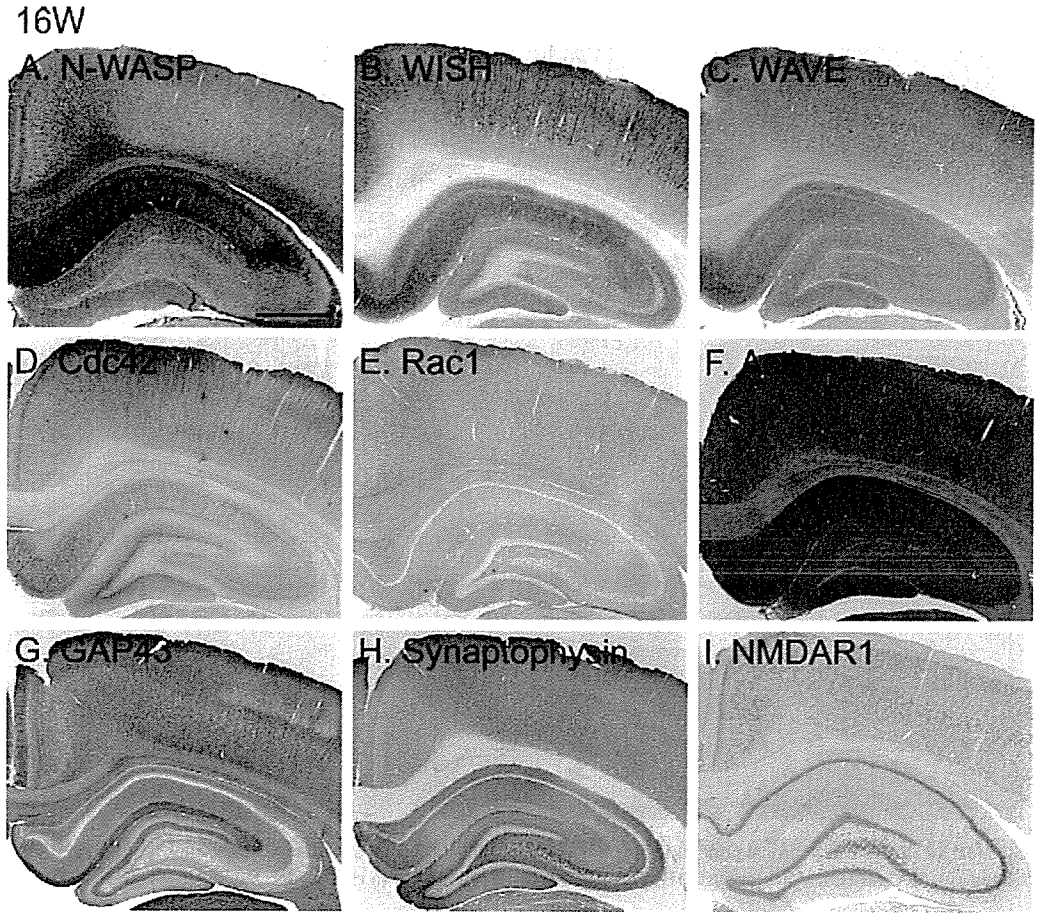

Fig. 5. Immunohistochemical localization of neuronal proteins in mature adult brains of 16-week-old rats. Immunoreactivities for N-WASP (A), WISH (B), WAVE (C), Cdc42 (D), Rac1 (E), actin (F), GAP43 (G), synaptophysin (H) and NMDAR1 (I) are shown in each panel. Scale bar = 1 mm.

In the 16-week-old brain (Fig. 6, lower panels), Cdc42 immunoreactivity was located moderately in the strata pyramidale and lacunosum-moleculare of CA1, and the middle and inner molecular layers and granule cell layer of DG, although there was less Cdc42 immunoreactivity in other regions (Fig. 6A). This immunoreactivity was also detected in dendrites of the stratum radiatum. WISH immunoreactivity was observed intensively in the strata oriens and radiatum of CA1 (Fig. 6B). The molecular layer of the DG appeared as a trilaminar pattern of WISH immunoreactivity, *i.e.*, the internal and external zones were moderate, whereas the middle zone was weak. In contrast, this immunoreactivity was not detected

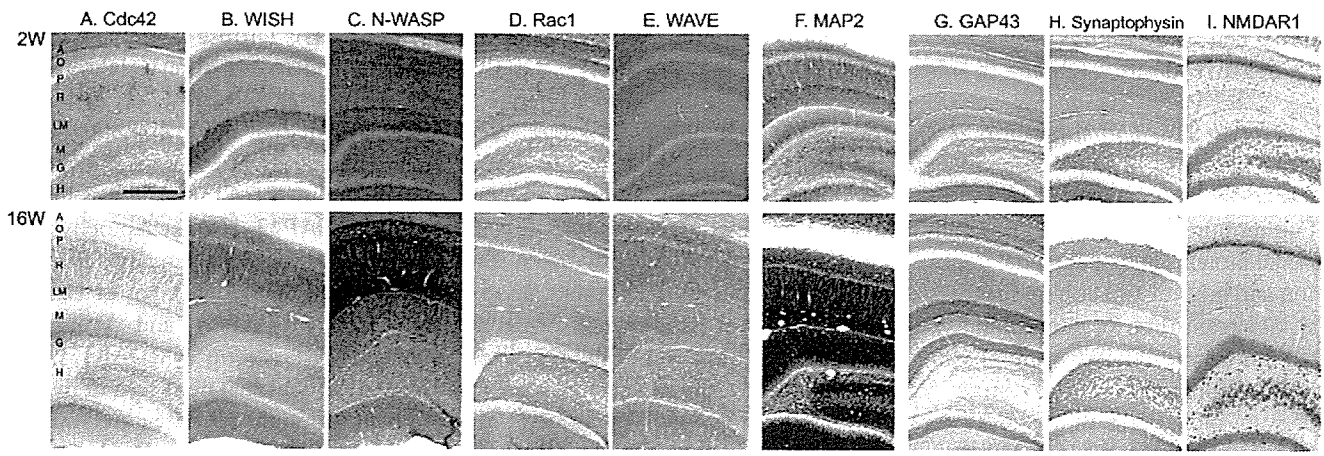

Fig. 6. Immunohistochemical localization of neuronal proteins in rat hippocampal laminar structures in CA1 and DG areas. Immunoreactivities for Cdc42 (A), WISH (B), N-WASP (C), Rac1 (D), WAVE (E), MAP2 (F), GAP43 (G), synaptophysin (H) and NMDAR1 (I) in hippocampal areas of 2-week-old (upper panels) and 16-week-old (lower panels) rat brains are shown at high magnification. Abbreviations: strata alveus (A), oriens (O), pyramidale (P), radiatum (R), lacunosum-moleculare (LM) of CA1, and molecular layer (M), granule cell layer (G), hilus (H) of DG. Scale bar = 400 μm.

in the strata alveus and pyramidale of CA1 and the granule cell layer of DG. N-WASP was strongly expressed in the strata oriens, pyramidale, radiatum and lacunosum-moleculare of CA1, and moderately throughout other regions (Fig. 6C). The immunoreactive area for Rac1 was detected throughout the hippocampus, except the stratum pyramidale of CA1 and the granule cell layer of DG where Rac1 expression was low (Fig. 6D). WAVE immunoreactivity was located intensively in the strata oriens and radiatum of CA1 and the inner molecular layer of DG, and other layers of the hippocampus showed homogenous labeling (Fig. 6E). Immunoreactivity of MAP2 was detected moderately in the stratum oriens of CA1, intensively in the stratum lacunosum-moleculare of CA1 and molecular layer of DG, and weakly in the stratum pyramidale of CA1 and granule cell layer of DG (Fig. 6F). MAP2 was strongly expressed in the apical dendrites of stratum radiatum of CA1. Immunoreactivity of MAP2 showed cancellous pattern in the hilus of DG. Similar to synaptophysin immunoreactivity, GAP43 immunoreactivity was little in the stratum pyramidale of CA1 and the granule cell layer of DG, and rich in the outer and inner zones of the molecular layer of DG (Fig. 6G and H). Additionally, the stratum lacunosum-moleculare contained abundant GAP43 (Fig. 6G). Immunoreactivity for synaptophysin was also observed intensively in the hilus of DG and weakly in the stratum lacunosum-moleculare of CA1, but it was not detected in the stratum alveus of CA1 (Fig. 6H). In contrast, dense immunoreactivity of NMDAR1 was restricted to the neuronal cells of stratum pyramidale of CA1 and the granule cell layer and hilus of DG, which was opposite to the synaptophysin expression pattern (Fig. 6I). Thus, the existence regions of N-WASP and WAVE were observed in the immunoreactive areas of their related molecules, and partially mimicked the immunoreactive areas of presynaptic markers in 16-week-old rat.

3.5. *Comparing the distributions of N-WASP, WISH and WAVE to those of presynaptic markers in CA1 subfield*

Numerous insights for synaptic structures and functions have been accumulated by investigating the hippocampal CA1 subfield, which have relatively simple anatomical structures and neuronal connections (Paxinos, 1995; Shepherd, 2004; Somogyi and Klausberger, 2005). Briefly, pyramidal neurons in the CA1 project basal dendrites to the stratum oriens and apical dendrites to the strata radiatum and lacunosum-moleculare. Projection from the CA3 to the CA1, *i.e.* glutamatergic Schaffer collaterals, forms synapses with dendritic arborization of principal neurons and interneurons, such as GABAergic basket cells and bistratified cells, in the strata oriens and radiatum, while projection from entorhinal cortex to the CA1 reaches the stratum lacunosum-moleculare of CA1. Interneurons also form synapses with principal neurons. In addition, thickness of the stratum radiatum of adult rat CA1 was increased compared to that of 2-week-old rat CA1 (data not shown), suggesting that synapses are markedly formed in the area during neuronal development. We, therefore, compared distributions of N-WASP, WAVE and WISH with those of presynaptic markers in the stratum radiatum of CA1 at higher magnification (Fig. 7).

In the stratum radiatum of 2-week-old rat hippocampal CA1 subfield (Fig. 7, upper panels), immunoreactivities for N-WASP, WISH and WAVE were detected entirely (Fig. 7A–C). MAP2 immunoreactivity was detected as a radial pattern (Fig. 7D). Immunoreactivities for GAP43 and synaptophysin were also observed widely in the area of the CA1 subfield (Fig. 7E and F). Thus, distribution patterns of N-WASP, WISH and WAVE were similar to those of presynaptic markers, such as GAP43 and synaptophysin in the 2-week-old rat stratum radiatum of the CA1 subfield.

In the stratum radiatum of 16-week-old rat CA1 subfield (Fig. 7, lower panels), immunoreactivities for N-WASP and WISH were observed in the neuropil and neurites (Fig. 7A and B). WAVE immunoreactivity was detected throughout the area of the CA1 subfield (Fig. 7C). While radial immunoreactivity of MAP2 was observed intensively in the dendrites (Fig. 7D), GAP43 and synaptophysin were expressed in neuropilar region (Fig. 7E and F). Therefore, N-WASP, WISH and WAVE were expressed in presynapse-like region of the 16-week-old rat stratum radiatum of the CA1 subfield.

In addition, we performed double immunolabeling analysis of WISH and GAP43 (Fig. 8). In 2-week-old rat, WISH immunoreactivity was colocalized with GAP43 immunoreactivity in, especially, the strata oriens, radiatum and lacunosum-moleculare of CA1, although there was various intensity more

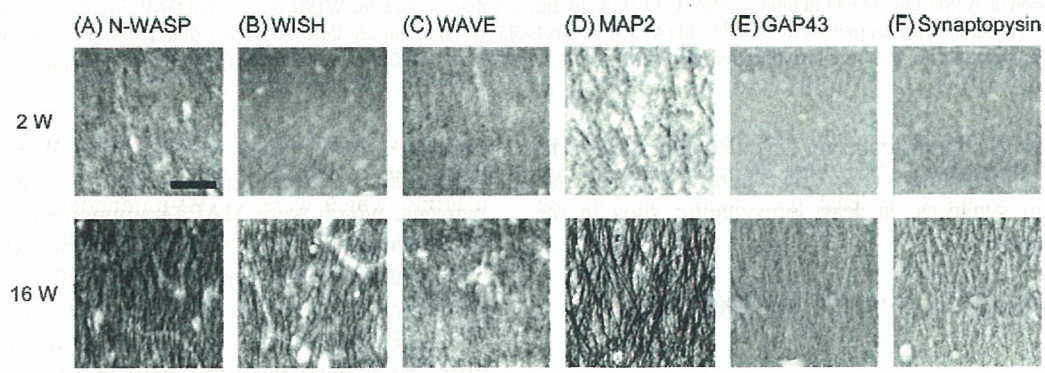

Fig. 7. Comparison of distributions of neuronal proteins in the stratum radiatum of CA1 at higher magnification. Immunoreactivities for N-WASP (A), WISH (B), WAVE (C), MAP2 (D), GAP43 (E) and synaptophysin (F) in stratum radiatum of 2-week-old (upper panels) and 16-week-old (lower panels) rat hippocampal CA1 subfield are shown at higher magnification. Scale bar = 50 μm.

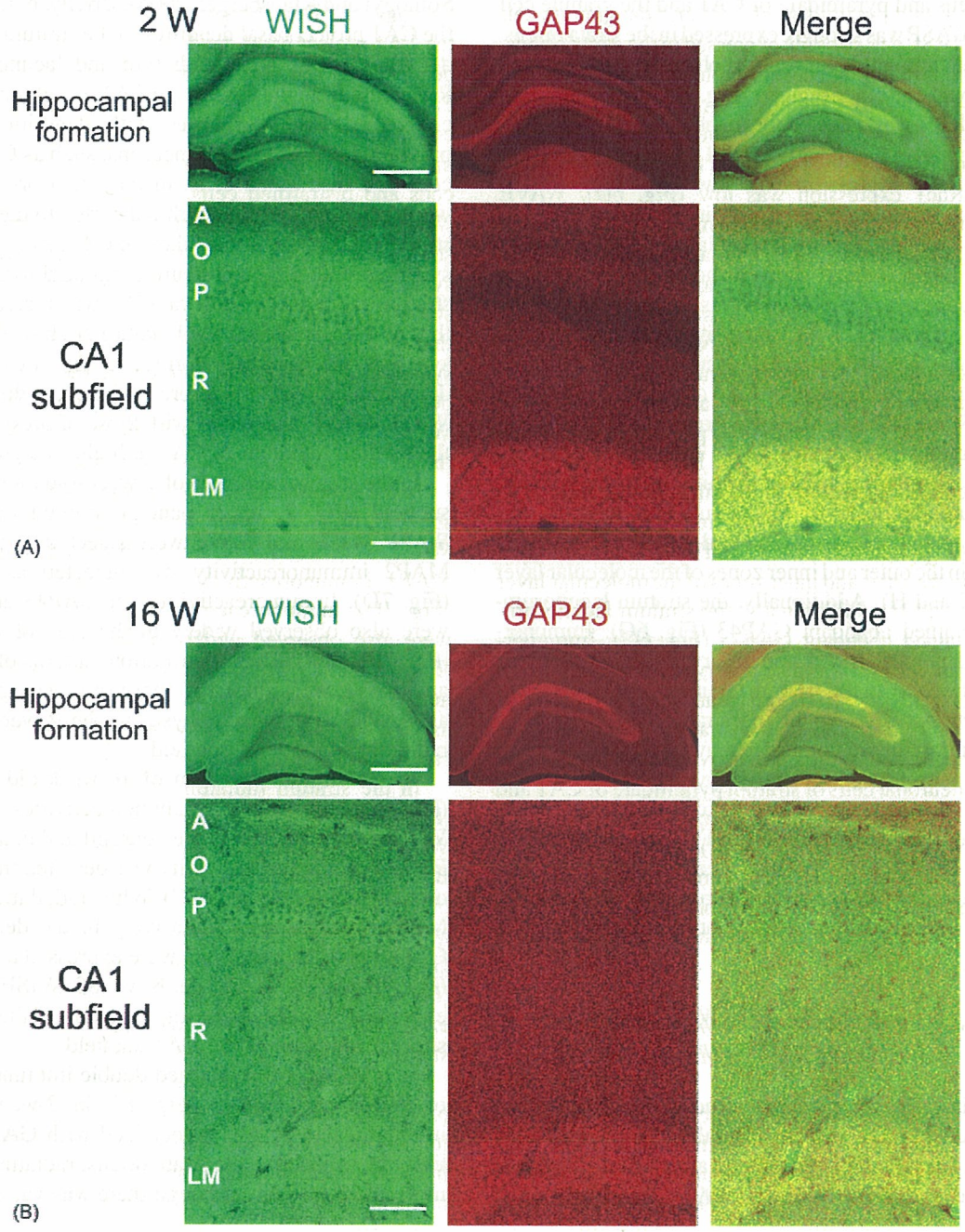

Fig. 8. Colocalization of WISH and GAP43 in hippocampal CA1 subfield. Immunofluorescence for WISH (green) and GAP43 (red) in the hippocampal formation (upper panels) and CA1 subfield (lower panels) of 2-week-old (A) and 16-week-old (B) rat brains are shown. Abbreviations in lower panels: strata alveus (A), oriens (O), pyramidale (P), radiatum (R) and lacunosum-moleculare (LM) of CA1. Scale bars = 400 μm (upper panels), 50 μm (lower panels).

or less (Fig. 8A). A similar tendency was also observed in the 16-week-old rat hippocampus (Fig. 8B). Therefore, WISH may be expressed in synapses, at least presynaptic sites in the hippocampal formation.

3.6. Distributions of N-WASP, WISH and WAVE in cultured neurons

During synaptic formation, filopodia are formed in growth cones and dendritic spines, in which F-actin is markedly constructed (Da Silva and Dotti, 2002). We furthermore examined distributions of N-WASP, WISH and WAVE in filopodial structures using cultured neurons. In cultured neurons, which were MAP2-immunopositive cells, filopodia-like multiple processes were formed and extended (Fig. 9). F-actin was distributed throughout the cell morphology, and was concentrated especially in leading edge of growing filopodia. N-WASP was located in cell body and neurites, and was markedly colocalized with F-actin in leading edges of filopodia (Fig. 9A). Immunoreactivities for WISH and WAVE were also observed throughout the cell, and were colocalized with F-actin in leading edges of processes (Fig. 9B and C). Therefore,

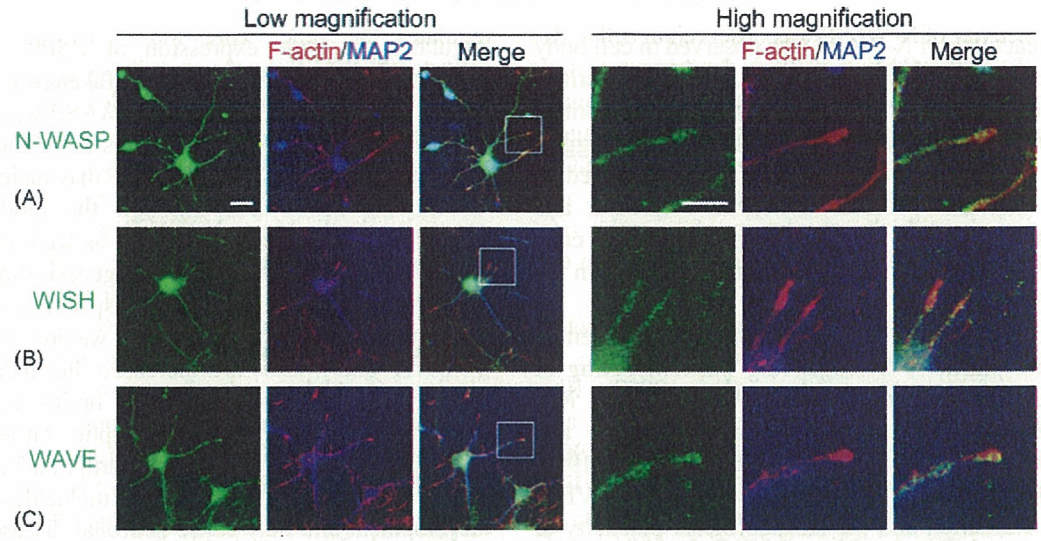

Fig. 9. Distributions of N-WASP, WISH and WAVE in rat cultured neurons. Neurons were immunocytochemically analyzed using an antibody (green) against N-WASP (A), WISH (B) or WAVE (C). Fluorescence for F-actin labeled by phalloidin (red) and MAP2 labeled by the antibody (blue) was also observed simultaneously. In addition, filopodial structures of a neuron are shown at high magnification. Scale bars = 20 μm in low magnification images, 10 μm in high magnification images.

N-WASP, WISH and WAVE may exist, at least, at leading edges of filopodial structures in cultured neurons.

4. Discussion

In the present study, we found that protein levels of N-WASP, WAVE and their related proteins such as Cdc42 and Rac1 were significantly increased in the membranous fractions of both the cerebral cortex and hippocampus in a development-dependent manner. In addition, actin protein was accumulated in the membranous fractions in a development-dependent manner, while actin in cytosolic fractions was decreased. It has been reported that N-WASP and WAVE are concentrated and activated beneath the plasma membrane where Cdc42, WISH and/or Rac1 are recruited and activated, resulting in dynamic membrane changes such as the formation of filopodium and lamellipodium (Miki et al., 1998a, 1998b; Fukuoka et al., 2001; Nakagawa et al., 2001; Etienne-Manneville and Hall, 2002). Actin is also enriched in the growth cone of elongating neurites and forms actin filaments with Arp2/3 complex which integrates actin cytoskeleton-regulatory factors such as N-WASP (Pollard and Borisy, 2003; Dent and Gertler, 2003). Therefore, it is suggested that N-WASP, WAVE and their related proteins are assembled in the cellular membrane of maturating neurons and facilitate actin filament formation, and consequently, the maturation of neuronal networks and functions.

In addition, we revealed that the distributions of N-WASP, WAVE and their related proteins in 2-week-old rat brain were relatively similar to those of GAP43 and synaptophysin, but opposite to that of NMDAR1. We also elucidated that immunoreactivities for N-WASP, WAVE and their related proteins appeared to distribute in GAP43- or synaptophysin-immunoreactive areas of 16-week-old brain. In the stratum radiatum of the CA1, N-WASP, WISH and WAVE immunoreactivities were also found in the neuropil which was GAP43- and synaptophysin-immunoreactive region. Moreover, WISH immunoreactivity was colocalized with GAP43 immunoreactivity in several areas of the hippocampus. GAP43 is expressed in the presynaptic terminal and synaptophysin is predominantly contained in presynaptic vesicles, and they contribute to synaptic function and plasticity (Benowitz and Perrone-Bizzozero, 1991; Masliah et al., 1991; Iwai et al., 1995). GAP43 is also concentrated in growth cones and enhances neurite outgrowth (Meiri and Gordon-Weeks, 1990; Dent and Gertler, 2003). In contrast, NMDAR1 is recognized as a postsynaptic receptor in the brain (Petralia et al., 1994). Many studies have shown that Rho family members essentially participate in all steps of neuronal sprouting, axonal guidance and synaptic formation through regulation of the actin cytoskeleton (Threadgill et al., 1997; Luo, 2002). A previous report suggests that N-WASP is an indispensable general regulator of the actin cytoskeleton for neurite extension in cultured neuronal cells (Banzai et al., 2000). Furthermore, WAVE exists in growth cones and dendritic spines of cultured neuronal cells (Nozumi et al., 2003; Pilpel and Segal, 2005). In fact, we observed the colocalization of N-WASP, WISH and WAVE with F-actin in the filopodia of cultured neurons. Thus, N-WASP, WAVE and related proteins may be localized in synapses, at least presynaptic sites such as axonal terminals of Schaffer collaterals. In contrast, immunoreactivities for N-WASP and WISH were also observed in dendrites of the stratum radiatum of CA1. It is reported that several subunits of glutamate receptors are expressed in many regions of hippocampal formation including dendrites of the stratum radiatum of CA1 (Hampson et al., 1992; Martin et al., 1993; Bradley et al., 1996), although NMDAR1 immunoreactivity was restricted to perikarya of principal neurons in the present study. Dendritic arborization of principal neurons which receives glutamatergic inputs is covered with massive spines (Shepherd, 2004). Therefore, it is likely that N-WASP and WISH are also localized in postsynaptic dendrites. In addition,

dense immunoreactivity of N-WASP was observed in cell body of pyramidal cells of the CA1 as well as dendritic neurites, which indicated that N-WASP biosynthesized in the somata may be transported to the neurites. These observations suggest that N-WASP, WAVE and related proteins are expressed in synaptic sites, and are involved in neurite outgrowth and synaptic formation through the regulation of growth cone motility, axonal guidance and dendritic spine formation in the developing brain.

On the other hand, the actin cytoskeleton plays essential roles in synaptic plasticity by regulating the remodeling of dendritic spines and synaptic structures (Luo, 2002). Rho family members also play their function to regulate and maintain the spines and synapses (Threadgill et al., 1997; Nakayama et al., 2000). Recently, the involvement of WAVE in dendritic spine formation and the morphological plasticity of neurons were reported (Pilpel and Segal, 2005). In addition, the presynaptic actin network is required for learning-related synaptic formation via the activation of Cdc42 and N-WASP (Udo et al., 2005). In the present study, we observed that the immunoreactivities for N-WASP and WAVE appeared to be in the synaptic sites. This result is congruent with the earlier observations described above. Thus, in the mature brain, N-WASP, WAVE and their related proteins located in synaptic sites may modulate and maintain synaptic plasticity and function. Interneurons as well as principal neurons are also contributed in synaptic function in the hippocampus (Shepherd, 2004; Somogyi and Klausberger, 2005). In developing brain, moderate immunoreactivities for N-WASP, WISH and WAVE were observed in the hilus of DG which contains GABAergic interneurons (Shepherd, 2004). In the hilus of mature hippocampal DG, immunoreactivities for N-WASP and WAVE were moderate while that for WISH was weak. Thus, interneurons in the hilus of DG, and probably in other regions of the hippocampus may express N-WASP and WAVE, as with principal neurons. In contrast, WISH may be expressed in both principal neurons and interneurons during development, but may be expressed predominantly in principal neurons of adult brain.

Three isoforms of WAVE proteins have been identified (Suetsugu et al., 1999). While WAVE2 is ubiquitously distributed in the body, WAVE1 and WAVE3 are predominantly expressed in the brain, and localized in growth cones of extending neurites (Suetsugu et al., 1999; Nozumi et al., 2003; Pilpel and Segal, 2005). Recently, WAVE1 knockout mice have been established. WAVE1 deletion demonstrates notable neuroanatomical hypoplasia and postnatal lethality (Dahl et al., 2003). In addition, loss of WAVE1 causes sensorimotor retardation and impairments of learning and memory in mice (Soderling et al., 2003); therefore WAVE, especially WAVE1, may be involved in normal maturation and the maintenance of neuronal networks, enlargement of the developing brain, and brain functions.

Knockout mice of N-WASP have also been established and show the severe abnormalities in neural tube and heart development, causing embryonic lethality (Snapper et al., 2001). It has been reported that nuclear N-WASP indirectly regulates the gene expression of HSP90 which stabilizes activated N-WASP (Suetsugu and Takenawa, 2003; Park et al., 2005). Our study revealed that N-WASP was also localized in the neuronal perikarya and neurites of developing and mature rat brain. Therefore, while N-WASP may maintain neurons and/or the nervous system through the modulation of gene expression in the brain, N-WASP, as well as WAVE, may be involved in developmental morphogenesis through cytoskeletal rearrangement in the brain under specific conditions, such as neuronal development. In contrast, we previously reported that N-WASP and WAVE are increased and located in abnormal neurites of Alzheimer's disease brains in which massive sprouting of neurites and synaptic failure are observed (Kitamura et al., 2003). Thus, disruption in the homeostasis of actin cytoskeleton-regulatory molecules impairs normal development and may cause neuronal diseases.

In conclusion, protein levels of N-WASP, WAVE and their related proteins were increased in a development-dependent manner. At that time, the translocation of actin from the cytosol to the membranous fraction was observed. Immunoreactivities for these proteins were widely but differentially distributed throughout the brain. In addition, N-WASP, WISH and WAVE appeared to be localized in synaptic sites, at least presynapse-like sites of developing and mature brain. Taken together, N-WASP, WAVE and their related factors may contribute to normal brain development and synaptic plasticity via the regulation of actin cytoskeleton.

Acknowledgements

This study was supported by the 21st Century Center of Excellence (COE) and Open Research Programs, and grants-in-aid from the Ministry of Education, Culture, Sports, Science and Technology of Japan and Takeda Science Foundation. D. Tsuchiya is a Research Fellow of the Japan Society for the Promotion of Science.

References

Banzai, Y., Miki, H., Yamaguchi, H., Takenawa, T., 2000. Essential role of neural Wiskott–Aldrich syndrome protein in neurite extension in PC12 cells and rat hippocampal primary culture cells. J. Biol. Chem. 275, 11987–11992.

Benowitz, L.I., Perrone-Bizzozero, N.I., 1991. The relationship of GAP-43 to the development and plasticity of synaptic connections. Ann. NY Acad. Sci. 627, 58–74.

Bishop, A.L., Hall, A., 2000. Rho GTPases and their effector proteins. Biochem. J. 348, 241–255.

Boyer, C., Schikorsky, T., Stevens, C.F., 1998. Comparison of hippocampal dendritic spines in culture and in brain. J. Neurosci. 18, 5294–5300.

Bradley, S.R., Levey, A.I., Hersch, S.M., Conn, P.J., 1996. Immunocytochemical localization of group III metabotropic glutamate receptors in the hippocampus with subtype-specific antibodies. J. Neurosci. 16, 2044–2056.

Dahl, J.P., Wang-Dunlop, J., Gonzales, C., Goad, M.E., Mark, R.J., Kwak, S.P., 2003. Characterization of the WAVE1 knock-out mouse: implications for CNS development. J. Neurosci. 23, 3343–3352.

Da Silva, J.S., Dotti, C.G., 2002. Breaking the neuronal sphere: regulation of the actin cytoskeleton in neuritogenesis. Nat. Rev. Neurosci. 3, 694–704.

Dickson, B.J., 2002. Molecular mechanisms of axon guidance. Science 298, 1959–1964.

Dent, E.W., Gertler, F.B., 2003. Cytoskeletal dynamics and transport in growth cone motility and axon guidance. Neuron 40, 209–227.

Eden, S., Rohatgi, R., Podtelejnkov, A.V., Mann, M., Kirschner, M.W., 2002. Mechanism of regulation of WAVE1-induced actin nucleation by Rac1 and Nck. Nature 418, 790–793.

Etienne-Manneville, S., Hall, A., 2002. Rho GTPases in cell biology. Nature 420, 629–635.

Fukuoka, M., Suetsugu, S., Miki, H., Fukami, K., Takenawa, T., 2001. A novel neuronal Wiskott–Aldrich syndrome protein (N-WASP) binding protein, WISH, induces Arp2/3 complex activation independent of Cdc42. J. Cell Biol. 152, 471–482.

Hampson, D.R., Huang, X.P., Oberdorfer, M.D., Goh, J.W., Auyeung, A., Wenthold, R.J., 1992. Localization of AMPA receptors in the hippocampus and cerebellum of the rat using an anti-receptor monoclonal antibody. Neuroscience 50, 11–22.

Harris, K.M., Jensen, F.E., Tsao, B., 1992. Three-dimensional structure of dendritic spines and synapses in rat hippocampus (CA1) at postnatal day 15 and adult ages: implications for the maturation of synaptic physiology and long-term potentiation. J. Neurosci. 12, 2685–2705.

Iwai, A., Masliah, E., Yoshimoto, M., Ge, N., Flanagan, L., de Silva, H.A., Kittel, A., Saitoh, T., 1995. The precursor protein of non-Aβ component of Alzheimer's disease amyloid is a presynaptic protein of the central nervous system. Neuron 14, 467–475.

Kitamura, Y., Tsuchiya, D., Takata, K., Shibagaki, K., Taniguchi, T., Smith, M.A., Perry, G., Miki, H., Takenawa, T., Shimohama, S., 2003. Possible involvement of Wiskott–Aldrich syndrome protein family in aberrant neuronal sprouting in Alzheimer's disease. Neurosci. Lett. 346, 149–152.

Luo, L., 2002. Actin cytoskeleton regulation in neuronal morphogenesis and structural plasticity. Annu. Rev. Cell Dev. Biol. 18, 601–635.

Martin, L.J., Blackstone, C.D., Levey, A.I., Huganir, R.L., Price, D.L., 1993. AMPA glutamate receptor subunits are differentially distributed in rat brain. Neuroscience 53, 327–358.

Masliah, E., Fagan, A.M., Terry, R.D., DeTeresa, R., Mallory, M., Gage, F.H., 1991. Reactive synaptogenesis associated by synaptophysin immunoreactivity is associated with GAP-43 in the dentate gyrus of the adult rat. Exp. Neurol. 113, 131–142.

Meiri, K.F., Gordon-Weeks, P.R., 1990. GAP-43 in growth cones is associated with areas of membrane that are tightly bound to substrate and is a component of a membrane skeleton subcellular fraction. J. Neurosci. 10, 256–266.

Miki, H., Miura, K., Takenawa, T., 1996. N-WASP, a novel actin-depolymerizing protein, regulates the cortical cytoskeletal rearrangement in a PIP2-dependent manner downstream of tyrosine kinases. EMBO J. 15, 5326–5335.

Miki, H., Sasaki, T., Takai, Y., Takenawa, T., 1998a. Induction of filopodium formation by a WASP-related actin-depolymerizing protein N-WASP. Nature 391, 93–96.

Miki, H., Suetsugu, S., Takenawa, T., 1998b. WAVE, a novel WASP-family protein involved in actin reorganization induced by Rac. EMBO J. 17, 6932–6941.

Miki, H., Yamaguchi, H., Suetsugu, S., Takenawa, T., 2000. IRSp53 is an essential intermediate between Rac and WAVE in the regulation of membrane ruffling. Nature 408, 732–735.

Nakagawa, M., Fukata, M., Yamaga, M., Itoh, N., Kaibuchi, K., 2001. Recruitment and activation of Rac1 by the formation of E-cadherin-mediated cell–cell adhesion sites. J. Cell Sci. 114, 1829–1838.

Nakayama, A.Y., Harms, M.B., Luo, L., 2000. Small GTPases Rac and Rho in the maintenance of dendritic spines and branches in hippocampal pyramidal neurons. J. Neurosci. 20, 5329–5338.

Nozumi, M., Nakagawa, H., Miki, H., Takenawa, T., Miyamoto, S., 2003. Differential localization of WAVE isoforms in filopodia and lamellipodia of the neuronal growth cone. J. Cell Sci. 116, 239–246.

Park, S.J., Suetsugu, S., Takenawa, T., 2005. Interaction of HSP90 to N-WASP leads to activation and protection from proteasome-dependent degradation. EMBO J. 24, 1557–1570.

Paxinos, G. (Ed.), 1995. The Rat Nervous System. 2nd ed. Academic Press, CA, USA.

Petralia, R.S., Yokotani, N., Wenthold, R.J., 1994. Light and electron microscope distribution of the NMDA receptor subunit NMDAR1 in the rat nervous system using a selective anti-peptide antibody. J. Neurosci. 14, 667–696.

Pilpel, Y., Segal, M., 2005. Rapid WAVE dynamics in dendritic spines of cultured hippocampal neurons is mediated by actin polymerization. J. Neurochem. 95, 1401–1410.

Pollard, T.D., Borisy, G.G., 2003. Cellular motility driven by assembly and disassembly of actin filaments. Cell 112, 453–465.

Shepherd, G.M. (Ed.), 2004. The Synaptic Organization of the Brain. 5th ed. Oxford University Press, NY, USA.

Snapper, S.B., Takeshima, F., Anton, I., Liu, C.H., Thomas, S.M., Nguyen, D., Dudley, D., Fraser, H., Purich, D., Lopez-Ilasaca, M., Klein, C., Davidson, L., Bronson, R., Mulligan, R.C., Southwick, F., Geha, R., Goldberg, M.B., Rosen, F.S., Hartwig, J.H., Alt, F.W., 2001. N-WASP deficiency reveals distinct pathways for cell surface projections and microbial actin-based motility. Nat. Cell Biol. 3, 897–904.

Soderling, S.H., Langeberg, L.K., Soderling, J.A., Davee, S.M., Simerly, R., Raber, J., Scott, J.D., 2003. Loss of WAVE-1 causes sensorimotor retardation and reduced learning and memory in mice. Proc. Natl. Acad. Sci. U.S.A. 100, 1723–1728.

Somogyi, P., Klausberger, T., 2005. Defined types of cortical interneurone structure space and spike timing in the hippocampus. J. Physiol. 562, 9–26.

Suetsugu, S., Miki, H., Takenawa, T., 1999. Identification of two human WAVE/SCAR homologues as general actin regulatory molecules which associate with the Arp2/3 complex. Biochem. Biophys. Res. Commun. 260, 296–302.

Suetsugu, S., Takenawa, T., 2003. Translocation of N-WASP by nuclear localization and export signals into the nucleus modulates expression of HSP90. J. Biol. Chem. 278, 42515–42523.

Takenawa, T., Miki, H., 2001. WASP and WAVE family proteins: key molecules for rapid rearrangement of cortical actin filaments and cell movement. J. Cell Sci. 114, 1801–1809.

Threadgill, R., Bobb, K., Ghosh, A., 1997. Regulation of dendritic growth and remodeling by Rho, Rac, and Cdc42. Neuron 19, 625–634.

Udo, H., Jin, I., Kim, J.H., Li, H.L., Youn, T., Hawkins, R.D., Kandel, E.R., Bailey, C.H., 2005. Serotonin-induced regulation of the actin network for learning-related synaptic growth requires Cdc42, N-WASP, and PAK in *Aplysia* sensory neurons. Neuron 45, 887–901.

Whitford, K.L., Dijkhuizen, P., Polleux, F., Ghosh, A., 2002. Molecular control of cortical dendrite development. Annu. Rev. Neurosci. 25, 127–149.

WILEY InterScience® DISCOVER SOMETHING GREAT

Journal of Neuroscience Research 85:153–165 (2007)

Presenilin 1 Is Involved in the Maturation of β-Site Amyloid Precursor Protein-Cleaving Enzyme 1 (BACE1)

Akira Kuzuya,[1] Kengo Uemura,[1] Naoyuki Kitagawa,[1] Nobuhisa Aoyagi,[1] Takeshi Kihara,[2] Haruaki Ninomiya,[3] Shoichi Ishiura,[4] Ryosuke Takahashi,[1] and Shun Shimohama[1]*

[1]Department of Neurology, Graduate School of Medicine, Kyoto University, Kyoto, Japan
[2]Department of Neuroscience for Drug Discovery, Graduate School of Pharmaceutical Sciences, Kyoto University, Kyoto, Japan
[3]Department of Neurobiology, Tottori University, Faculty of Medicine, Yonago, Japan
[4]Department of Life Sciences, Graduate School of Arts and Sciences, University of Tokyo, Tokyo, Japan

One of the pathologic hallmarks of Alzheimer's disease is the excessive deposition of β-amyloid peptides (Aβ) in senile plaques. Aβ is generated when β-amyloid precursor protein (APP) is cleaved sequentially by β-secretase, identified as β-site APP-cleaving enzyme 1 (BACE1), and γ-secretase, a putative enzymatic complex containing presenilin 1 (PS1). However, functional interaction between PS1 and BACE1 has never been known. In addition to this classical role in the generation of Aβ peptides, it has also been proposed that PS1 affects the intracellular trafficking and maturation of selected membrane proteins. We show that the levels of exogenous and endogenous mature BACE1 expressed in presenilin-deficient mouse embryonic fibroblasts (PS−/−MEFs) were reduced significantly compared to those in wild-type MEFs. Moreover, the levels of mature BACE1 were increased in human neuroblastoma cell line, SH-SY5Y, stably expressing wild-type PS1, compared to native cells. Conversely, the maturation of BACE1 was compromised under the stable expression of dominant-negative mutant PS1 overexpression. Immunoprecipitation assay showed that PS1 preferably interacts with proBACE1 rather than mature BACE1, indicating that PS1 can be directly involved in the maturation process of BACE1. Further, endogenous PS1 was immunoprecipitated with endogenous BACE1 in SH-SY5Y cells and mouse brain tissue. We conclude that PS1 is directly involved in the maturation of BACE1, thus possibly functioning as a regulator of both β- and γ-secretase in Aβ generation.

Key words: Alzheimer's disease; amyloid; γ-secretase; β-secretase

Alzheimer's disease (AD) is pathologically characterized by the excessive accumulation and deposition of β-amyloid peptides (Aβ) (Kang et al., 1987). Because the longer Aβ peptide species, Aβ1-42 (Aβ42), aggregates more readily than the shorter and more predominant species, Aβ1-40 (Aβ40), it is believed that Aβ42 plays an important role in AD pathogenesis (Hardy, 1997a,b). Aβ peptides are generated by the consecutive proteolysis of β-amyloid precursor protein (APP), by distinct enzymatic moieties known as β-secretase and γ-secretase (Golde et al., 1993; Haass et al., 1993). Recently, primary β-secretase in the brain was identified as a membrane-associated aspartyl protease, β-site APP-cleaving enzyme 1 (BACE1) (Hussain et al., 1999; Sinha et al., 1999; Vassar et al., 1999; Yan et al., 1999; Haniu et al., 2000). BACE1 generates a membrane-bound APP C-terminal fragment (APP CTFβ), which undergoes intra-membranous γ-secretase cleavage to generate the Aβ peptide. Although multiple lines of biochemical and genetic evidence have shown that γ-secretase forms high molecular weight complexes containing at least presenilin 1 (PS1), nicastrin, aph-1, and pen-2 (Capell et al., 1998; Yu et al., 2000; Edbauer et al., 2002; Francis et al., 2002; Lee et al., 2002; Steiner et al., 2002; Gu et al., 2003), the functional interaction of β- and γ-secretase in Aβ generation still remains unclear.

Importantly, mutations in PS1 are the most common known cause of autosomal dominant familial Alzheimer's disease (FAD) (Rogaev et al., 1995; Sherrington et al., 1995; Thinakaran 1999). These mutations increase the level of Aβ42/40 in transfected mammalian cells and the

Contract grant sponsor: Ministry of Education, Culture, Sports, Science and Technology of Japan; Contract grant sponsor: Japan Society for the Promotion of Science; Contract grant sponsor: Ministry of Health, Labour and Welfare of Japan; Contract grant sponsor: Smoking Research Foundation; Contract grant sponsor: Philip Morris USA, Inc.; Contract grant sponsor: Philip Morris International.

*Correspondence to: Dr. Shimohama, Department of Neurology, Graduate School of Medicine, Kyoto University, 54 Shogoin-Kawaharacho, Sakyo-ku, Kyoto 606-8507, Japan.
E-mail: i53367@sakura.kudpc.kyoto-u.ac.jp

Received 20 January 2006; Revised 25 May 2006; Accepted 4 September 2006

Published online 30 October 2006 in Wiley InterScience (www.interscience.wiley.com). DOI: 10.1002/jnr.21104

brains of transgenic mice (Borchelt et al., 1996; Duff et al., 1996). Whereas it has generally been accepted that PS1 is the essential catalytic component of γ-secretase (Wolfe et al., 1999a,b), it has also been reported that Aβ is still generated in absence of both PS1 and its homologue PS2 (Armogida et al., 2001; Wilson et al., 2002). In addition, it has also been proposed that PS1 affects the intracellular trafficking and maturation of selected membrane proteins. Indeed, PS1 deficiency affects the intracellular trafficking and maturation of TrkB, as well as ICAM5/telenchephalin in neurons (Naruse et al., 1998; Annaert et al., 2001). We have also shown that PS1 regulates the intracellular trafficking and maturation of N-cadherin in SH-SY5Y cells (Uemura et al., 2003a). Furthermore, it has been shown that PS1 is involved in regulating the intracellular trafficking and maturation of APP and nicastrin, which are essential for Aβ generation (Kim et al., 2001; Edbauer et al., 2002; Leem et al., 2002a,b; Cai et al., 2003; Herreman et al., 2003). Although there is no reported genetic linkage between mutations in BACE1 and AD to date, recent reports have shown an elevation of BACE1 protein expression and its enzymatic activity in AD brains (Fukumoto et al., 2002; Holsinger et al., 2002; Yang et al., 2003), indicating that BACE1, as well as PS1, is involved significantly in AD pathogenesis. Recently, Kamal et al. (2001) showed that APP, PS1, and BACE1 are transported in the same membrane vesicles along the axons in vivo, via the direct binding of APP to the kinesin light chain subunit of kinesin-I, a microtubule motor protein. These observations raise the possibility that PS1 is related functionally to the intracellular trafficking and maturation of BACE1 through the amyloidogenic pathway of APP.

Based on the above observations, we hypothesized that PS1 influences the intracellular trafficking and maturation of BACE1. To characterize the effect of PS1 on the trafficking-dependent maturation of BACE1, wild-type (wt) and presenilin-deficient mouse embryonic fibroblast cell lines (MEFs) or human neuroblastoma SH-SY5Y cell lines stably expressing either wt PS1 or dominant-negative PS1 were used in the present study. We report that wt PS1 binds BACE1 directly and upregulates its maturation, whereas the absence of PS1 or dominant-negative PS1 downregulates its maturation. Taking the previous reports and our results together, we suggest that PS1 significantly modulates both β- and γ-secretase via regulation of the intracellular trafficking of both secretase, and operates as a primary regulator determining the amyloidogenic processing of APP.

MATERIALS AND METHODS

Cell Cultures, Constructs, Transfection and Brain Tissue

The generation of SH-SY5Y cells stably expressing either wild-type PS1 (wt PS1) or dominant-negative (D385A) PS1 has been described previously (Uemura et al., 2003b). In the present experiments, we used native SH-SY5Y cells as control cells. Wild-type (wt) and PS1/PS2 (PS−/−) double knockout mouse embryonic fibroblast (MEF) cell lines (Herreman et al., 1999, 2003) were kindly provided by Dr. De Strooper (Center for Human Genetics, KUL, VIB, Belgium). These cell lines were maintained in Dulbecco's modified Eagle's medium (DMEM; Nissui Pharmaceutical, Tokyo, Japan) containing 10% fetal bovine serum (FBS), 100 IU/ml penicillin, 100 μg/ml streptomycin and glutamine (2 mM) (Life Technologies, Rockville, MD) at 37°C in 5% CO_2. Stably transfected SH-SY5Y cells were selected and maintained with 300 mg/ml G418 (Wako Pure Chemical Industries, Ltd., Osaka, Japan). For immunoprecipitation experiment using the SH-SY5Y cell lines, the cells were cultured in Opti-MEM I (Gibco BRL, Rockville, MD) containing 10% FBS to grow at full confluency. An expression vector to encode HA-tagged human full-length BACE1 has been described previously (Hattori et al., 2002). An expression vector to encode FAD-linked PS1 mutant containing proline (Pro) to leucine mutation at position Pro-117 (P117L PS1) has been described previously (Uemura et al., 2003b). An expression vector to encode GFP was purchased from Invitrogen. Lipofectamine 2000 (Invitrogen Life Technologies) was used for transient cotransfection of BACE1 and GFP constructs into MEF cells, according to the instruction. During and after the transfection, cells were maintained in Opti-MEM I. GFP was cotransfected with BACE1, using as an indicator of transfection efficiency. To obtain comparable expression levels of GFP between wt and PS−/− MEF cells, the transfection condition was optimized by varying doses of DNA and Lipofectamine 2000. Rat primary cultures were obtained from the fetal rat cerebral cortex (17–19 days gestation) and were maintained as described previously (Kihara et al., 1997). Mouse primary cultures were prepared as described previously (Uemura et al., 2006). Only mature neurons were used for the present experiments. For the treatment of γ-secretase inhibitors to primary cultures, the medium containing either 2 μM L-685,458 or 1 μM DAPT were exchanged every day for 4 days. Control cells were treated with vehicle (DMSO) only. Fresh brain tissue was prepared from 3-month-old mice. The animals were treated in accordance with the guidelines published in the National Institutes of Health Guide for the Care and Use of Laboratory Animals.

Antibodies and Reagents

Monoclonal antibody MAB5308 against the C terminus of BACE1, monoclonal antibody MAB5232 against the loop domain of PS1 and rabbit polyclonal anti-mannosidase II antibody were purchased from Chemicon (Temecula, CA). Monoclonal and rabbit polyclonal anti-HA antibodies, monoclonal anti-β-actin antibody, rabbit polyclonal anti-APP antibody recognizing the C terminus and rabbit polyclonal anti-BACE1 antibody, EE-17, recognizing the N terminus (amino acids 46–62), were purchased from Sigma (St. Louis, MO). Rabbit polyclonal anti-proBACE1 antibody (targeting amino acids 26–45 corresponding to the prodomain sequence), rabbit polyclonal anti-BACE1 antibody (targeting amino acids 485–501) and rabbit polyclonal anti-BACE1 antibody (targeting amino acids 487–501) were purchased from Calbiochem. Rabbit polyclonal anti-calnexin antibody was purchased from StressGen (Victoria, BC). Rabbit polyclonal anti-PS1 antibody against the N terminus was purchased from Santa Cruz Biotechnology (Santa Cruz, CA). Rabbit polyclonal anti-GFP antibody was purchased from

TABLE I. Antibodies used in Experiment

Antigen	Name	Epitope	Host
BACE1	MAB5308	C-terminus	Monoclonal
	Anti-BACE1	C-terminus (aa 487–501)	Polyclonal rabbit
	Anti-BACE1	C-terminus (aa 485–501)	Polyclonal rabbit
	EE-17	N-terminus (aa 46–62)	Polyclonal rabbit
	Anti-proBACE1	Prodomain (aa 26–45)	Polyclonal rabbit
PS1	Anti-PS1	N-terminus	Polyclonal rabbit
	MAB5232	Loop domain	Monoclonal

Molecular Probes (Eugene, OR). For immunostaining, Alexa Fluor 546 goat anti-mouse IgG (H+L) conjugate and Alexa Fluor 488 goat anti-rabbit IgG (H+L) conjugate (Molecular Probes) were used as secondary antibodies. In Table I, the corresponding epitopes of anti-PS1 and anti-BACE1 antibodies used in the present experiment are summarized. Two well-characterized γ-secretase inhibitors, L-685,458 and *N*-[*N*-(3,5-difluorophenacetyl)-L-alanyl]-*S*-phenylglycine *t*-butyl ester (DAPT) were purchased from Sigma and Calbiochem, respectively.

Reverse Transcription-Polymerase Chain Reaction

Total RNA was extracted from confluent cells of each cell line by using ISOGEN (Nippon Gene, Toyama, Japan). Equal amounts of total RNA obtained from each cell line were processed for cDNA synthesis using oligo (dT) primers and reverse transcriptase, using a RNA LA PCR kit (AMV) (TaKaRa, Tokyo, Japan). They were amplified by polymerase chain reaction (PCR) using sense and anti-sense primers specific for either the human *BACE1* gene (5′CATTGGAGGTATCGACCACTCGCT3′ and 5′CCACAGTCTTCCATGTCCAA-GGTG3′, the product size was 624 bp; GenBank accession number AF190725) or the human *glyceraldehyde-3-phosphate dehydrogenase* (*GAPDH*) gene (5′ACCACAGTCCATGCCATCAC3′ and 5′TCCACCACCCTGTTGCTGTA3′, 452 bp; J04038). The amplification program consisted of a denaturing step at 94°C for 1 min, an annealing step at 62°C for 40 src, and an extension step at 72.9°C for 50 sec. This was repeated 25 cycles for BACE and 18 cycles for GAPDH. The PCR products separated on a 1.5% agarose gel were stained by ethidium bromide and visualized using a UV transilluminator coupled to a CCD camera.

Preparation of Protein Samples, Western Blot Analysis, and immunoprecipitation

Confluent cells were rinsed three times with ice-cold phosphate-buffered saline (PBS) and centrifuged. Each pellet was suspended in TNE buffer (10 mM Tris-Hcl, pH 7.8, 1% NP40, 0.15 M NaCl, 1 mM EDTA) supplemented with 1 mM dithiothreitol (DTT) and 1 mM phenylmethylsulphonyl fluoride (PMSF), dispersed by pipetting vigorously 20 times and then rotated for 1 hr at 4°C. Each sample was then centrifuged at 25,000 × *g* for 30 min at 4°C and the supernatants were collected to obtain the protein samples. Protein concentration was determined using the Bradford assay (Bradford, 1976). Equal amounts of protein were treated with Protein G-Sepharose (Amersham Biosciences, Uppsala, Sweden) overnight at 4°C. After removing Protein G-Sepharose by centrifugation at 2,000 × *g* for 5 min, either the MAB5308 antibody, the anti-BACE1 antibody (Calbiochem), or anti-PS1 antibody (Santa Cruz Biotechnology, Santa Cruz, CA) was added to the lysate. Each sample was rotated for 1 hr at 4°C and then treated with Protein G-Sepharose for 1 hr at 4°C. The immunoprecipitates were washed with TNE buffer five times and resuspended in 2× sample buffer (125 mM Tris-HCl [pH 6.8], 4.3% SDS, 30% glycerol, 10% 2-mercaptoethanol, and 0.01% bromophenol blue). After boiling for 3 min, the supernatants were subjected to Western blotting. For the detection of full-length PS1, the suspension was incubated at 37°C for 10 min instead of boiling. Alternatively, confluent cells were rinsed three times with ice-cold PBS and scraped off. Cell pellets were suspended in TNE buffer supplemented with 1 mM DTT and 1 mM PMSF, and sonicated. The samples were centrifuged at 25,000 × *g* for 30 min at 4°C and the supernatants were collected to obtain protein samples. Protein concentration was determined using the Bradford assay, and then equal amounts of cell extracts were subjected to Western blotting.

In Western blot analysis, samples were electrophoresed on polyacrylamide gels in the presence of SDS. Immunoblotting was carried out by transferring the proteins to polyvinylidene difluoride microporous membrane, which was then blocked with 5% skimmed milk in 10 mM PBS containing 0.1% Tween 20 (PBS-T), and incubated with the primary antibodies in PBS-T containing 4% BSA overnight at 4°C. The membranes were then washed in PBS-T and incubated with a horseradish peroxidase-conjugated anti-mouse or anti-rabbit IgG (Amersham, Little Chalfont, UK) in PBS-T for 1 hr at room temperature. The specific reaction was visualized, using the enhanced chemiluminescence method (ECL) (Amersham).

Immunostaining

Immunostaining was carried out as described previously (Uemura et al., 2003b). Briefly, SH-SY5Y cell lines and 5 days in vitro primary cultures were fixed with 4% paraformaldehyde for 20 min. Fixed cells were blocked with 3% BSA in PBS with 0.2% Triton X-100 for 15–20 min and incubated overnight at 4°C with primary antibodies diluted in PBS containing 3% BSA. Immunoreactivity was visualized using the species-specific secondary antibodies mentioned above. Samples were observed using a LSM (Zeiss) confocal scanning microscope.

Statistical Analysis

The relative density of the bands in RT-PCR or Western blot was analyzed by quantitative densitometry using a computerized image analysis program (NIH Image 1.59). To compare either the levels of mature BACE1 or the mature:proBACE1 ratio among the SH-SY5Y cell lines, statistical analysis was carried out using one-way ANOVA, followed by post-hoc Fisher's protected least significant difference. To compare the mature BACE1:GFP ratio or the mature:proBACE1 ratio between wt MEFs and PS−/− MEFs, statistical analysis was carried out using Student's *t*-test. Data were expressed as the mean ± SD, and significance was assessed at $P < 0.01$.

RESULTS

PS1 Is Involved in BACE1 Maturation

Previous studies showed that BACE1 undergoes core glycosylation in the endoplasmic reticulum (ER) cotranslationally, and is produced as proBACE1. Then, short-lived proBACE1 is transported from the ER to the Golgi apparatus, and undergoes rapid maturation by the proteolytic removal of the prodomain followed by complex *N*-glycosylation in the Golgi apparatus (Capell et al., 2000; Haniu et al., 2000; Huse et al., 2000; Creemers et al., 2001). Finally, mature BACE1 is quite stable unlike proBACE1, and is located in the late secretory compartments, the plasma membrane, and the endosomal compartments (Huse et al., 2000; Walter et al., 2001).

To examine a possible role for PS1 in regulating BACE1 maturation, we first investigated the effect of PS deficiency on BACE1 maturation, using PS1 and its homologue PS2 double-knockout (PS−/−) mouse embryonic fibroblasts (MEFs) (Herreman et al., 1999, 2003). HA-tagged wt BACE1 and GFP plasmids were transiently cotransfected into wt and PS−/− MEFs, and the cells were collected 24 hr after transfection. Each cell lysate was subjected to Western blot analysis using either monoclonal anti-HA antibody or anti-GFP antibody. As shown in Figure 1A, the immunoblotting bands of HA-tagged BACE1 were detected as two different molecular weight bands. The higher molecular weight bands represented mature BACE1, complex N-glycosylated one, whereas the lower molecular weight bands represented proBACE1, a precursor of mature BACE1 (Capell et al., 2000). Interestingly, the levels of mature BACE1 were apparently reduced in PS−/− MEFs compared to wt MEFs, whereas the levels of GFP were comparable between them, indicating that the transfection efficiency was not different (Fig. 1A). Quantitative analysis showed that the ratio of mature BACE1:GFP was reduced by 70% in PS−/− MEFs, compared to that in wt MEFs (Fig. 1B; $n = 4$, $P < 0.0005$). In addition, the ratio of mature:proBACE1 was reduced by 50% in PS−/− MEFs, compared to that in wt MEFs (Fig. 1C, $n = 4$, $P < 0.0005$). These data suggest that the expression level of PS affects significantly the maturation of BACE1 in MEF cells. To further confirm the effect of PS expression on BACE1 maturation at endogenously expressed level, we compared the levels of endogenous BACE1 between wt and PS−/− MEFs. Equal amounts of cell lysates obtained from wt and PS−/− MEFs were subjected to Western blotting, using anti-BACE1 antibody (targeting amino acid 485–501), and anti-proBACE1 antibody. Lysates of mouse brain tissue and mouse primary neurons were used as positive controls. As expectedly, the level of mature BACE1 in PS−/− MEFs was reduced drastically as compared to that in wt MEFs, whereas the levels of β actin were almost constant between them (Fig. 1D). Interestingly, we observed no significant difference in the levels of proBACE1 between them, indicating that the maturation of endogenous BACE1 was remarkably inhibited in PS−/− MEFs as compared to in wt MEFs (Fig. 1D). We then asked whether the maturation of exogenously expressed BACE1 is affected by co-expression of either wt PS1 or P117L PS1 mutant causing FAD. Plasmids to encode either GFP, wt PS1, or P117L PS1 were cotransfected with HA-tagged BACE1 plasmid into PS−/− MEFs by 1:1 ratio. The cells were collected 24 hr after transfection, and each cell lysate was subjected to Western blotting analysis using either rabbit polyclonal anti-HA antibody or anti-PS1 antibody (against the N terminus). As shown in Figure 1E, the levels of mature and proBACE1 were increased drastically in the cells expressing either wt PS1 or P117L PS1 as compared to those in the cells expressing GFP, whereas the levels of wt PS1 and P117L PS1 were almost similar. This result suggests that both wt PS1 and P117L PS1 similarly upregulate the stability of both mature and proBACE1 in this experimental system. The above data suggest that the expression level of PS is involved significantly in the stabilization and maturation of BACE1 in MEF cells.

To examine a specific role for PS1 in BACE1 maturation in neuronal cells, we used SH-SY5Y cells stably expressing either wild-type PS1 (wt PS1) or PS1 containing aspartate (Asp) to alanine mutation at position Asp-385 (D385A PS1). As described previously, exogenous overexpression of D385A PS1 that fails to undergo endoproteolysis, significantly replaces endogenous PS1 and results in a dominant negative version of PS1 in SH-SY5Y cells (Uemura et al., 2003b). To specifically identify either proBACE1 or mature BACE1, equal amounts of cell lysate obtained from each cell line were subjected to Western blotting using the anti-proBACE1 antibody (targeting amino acids 26–45 corresponding to the prodomain sequence) and the antibody EE-17 (targeting amino acids 46–62 corresponding to the neoepitope after removal of the prodomain), respectively. It has been reported that neoepitope antibodies specific for BACE1 after removal of the prodomain preferentially recognize the mature BACE1 polypeptide (Capell et al., 2000). Indeed, the antibody EE-17 detected the mature BACE1 polypeptide in a higher molecular weight band of 70–75 kDa that represented its complex *N*-glycosylation, whereas the anti-proBACE1 antibody detected the proBACE1 polypeptide in a tighter band of 65 kDa in lysates from each cell line (Fig. 2A). These results are consistent with the molecular weight of BACE1 described previously (Vassar et al., 1999; Capell et al., 2000; Pinnix et al., 2001). Quantitative analysis showed that the amount of mature BACE1 was increased by 20% in wt PS1 cells and was reduced by 50% in D385A PS1 cells, compared to that in control cells (Fig. 2B; $n = 3$, $\#P < 0.01$ vs. control, $\star P < 0.0001$). Interestingly, the ratio of mature:proBACE1 was reduced significantly by 60% in D385A PS1 cells, compared to that in control cells, whereas it was not statistically different between control and wt PS1 cells (Fig. 2C; $n = 3$, $\star P < 0.001$ vs. control).

To investigate whether the difference in BACE1 protein levels among these cell lines is dependent on the mRNA expression levels, the level of BACE1 mRNA expression in these cell lines was quantitated by semi-quantitative reverse transcription-polymerase chain reaction (RT-PCR) analysis. Expression of both BACE1 mRNA

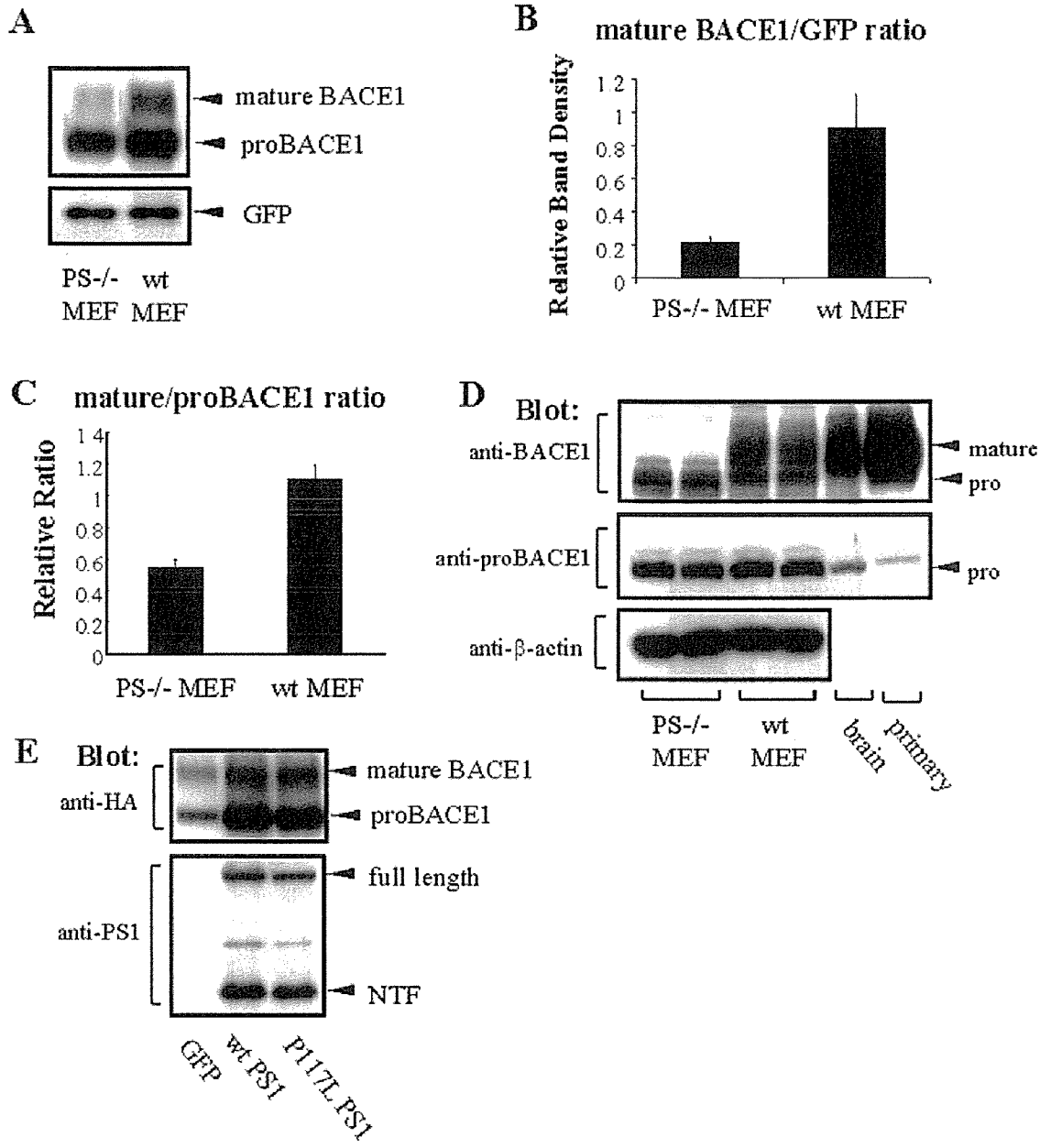

Fig. 1. PS1 is involved in BACE1 maturation post-translationally. **A:** HA-tagged BACE1 and GFP cDNA were transiently cotransfected into mouse embryonic fibroblasts (MEFs) derived from either wild-type (wt) or PS1/PS2 double-knockout (PS−/−) mice. Twenty-four hours after transfection, the cells were collected and each cell lysate was subjected to Western blot analysis and probed by either monoclonal anti-HA antibody or anti-GFP antibody. The level of mature BACE1 was apparently decreased in PS−/− MEFs as compared to that in wt MEFs, whereas the levels of GFP were almost similar between them. One representative immunoblot is shown. **B:** The band densities of either mature BACE1 or control GFP in four independent experiments were quantified by NIH imaging. The ratio of mature BACE1:GFP was calculated and analyzed by Student's *t*-test. The ratio of mature BACE1:GFP in PS−/− MEFs was significantly reduced, compared to that in wt MEFs ($n = 4$, $P < 0.0005$). **C:** The ratio of mature:proBACE1 was quantified by NIH imaging and analyzed by Student's *t*-test. The ratio of mature BACE1:proBACE1 in PS−/− MEFs was apparently reduced, compared to that in wt MEFs ($n = 4$, $P < 0.0005$). **D:** Equal amounts of cell lysates obtained from wt and PS−/− MEFs were subjected to Western blotting using the indicated antibodies. Lysates of mouse brain tissue and mouse primary neurons were used as positive controls. The endogenous level of mature BACE1 was drastically reduced in PS−/− MEFs as compared to those in wt MEFs, whereas the levels of proBACE1 were almost constant between them. One representative immunoblot is shown. **E:** Plasmids to encode either GFP, wt PS1, or P117L PS1 were cotransfected with HA-tagged BACE1 plasmid into PS−/− MEFs by 1:1 ratio. Each cell lysate was subjected to Western blotting analysis using the indicated antibodies. The levels of mature and proBACE1 were drastically increased in the cells expressing either wt PS1 or P117L PS1 as compared to those in the control cells. One representative immunoblot is shown.

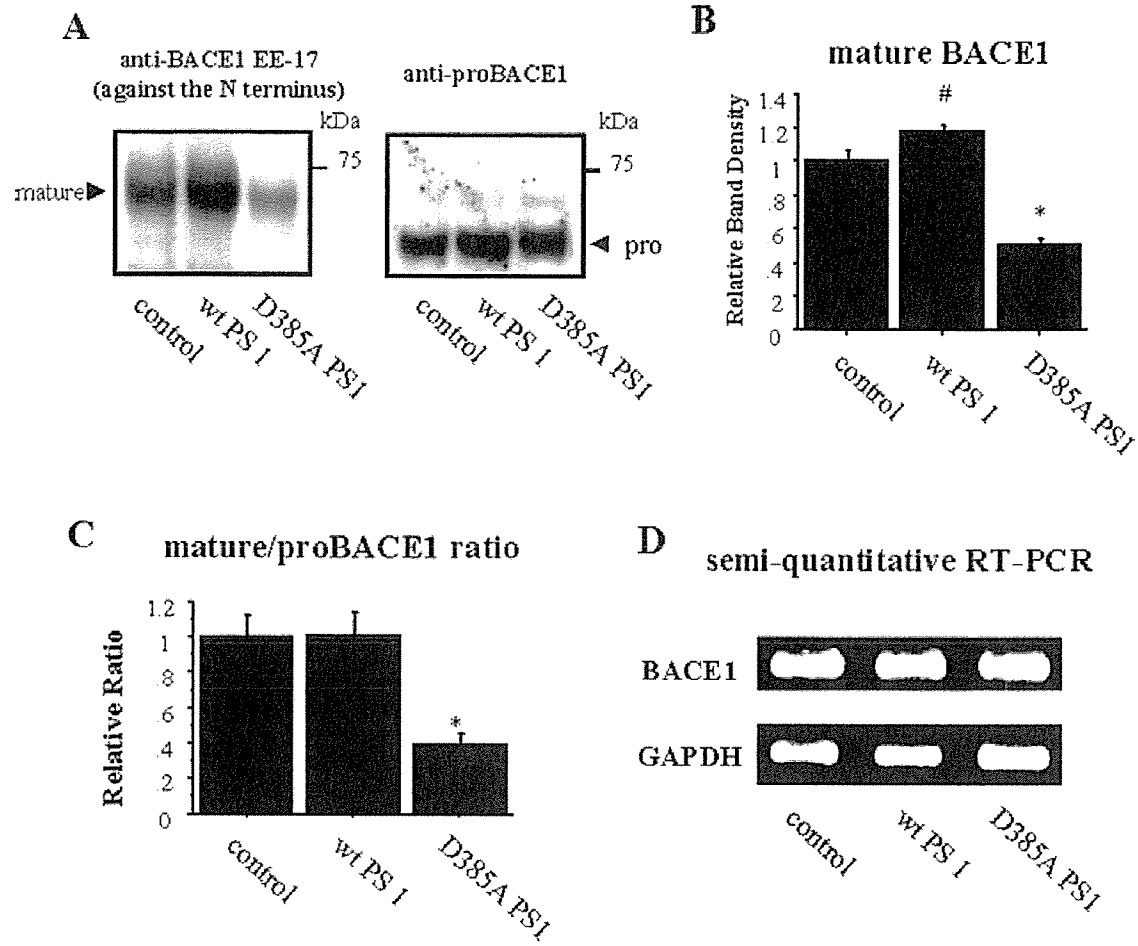

Fig. 2. **A:** Protein levels of BACE1 were compared between control SH-SY5Y cells and SH-SY5Y cells stably expressing either wt PS1 or D385A PS1. Equal amounts of whole cell lysates were subjected to Western blotting using the indicated antibodies. Mature BACE1 polypeptide was identified as a higher band of 70–75 kDa, whereas pro-BACE1 polypeptide was identified as a tighter band of 65 kDa. **B:** Immunoblotting of the mature BACE1 in each cell line was quantified by NIH imaging and analyzed by one-way ANOVA. The level of mature BACE1 was significantly reduced in D385A PS1 cells and increased in wt PS1 cells ($n = 3$, $^{\#}P < 0.01$ vs. control, $^{*}P < 0.0001$). **C:** The ratio of mature:proBACE1 in each cell line was quantified by NIH imaging and analyzed by one-way ANOVA. The ratio of mature:proBACE1 in D385A PS1 cells was significantly reduced ($n = 3$, $P < 0.001$ vs. control). **D:** The representative data of semi-quantitative RT-PCR analysis are shown. The processed cDNA was amplified by PCR using primers specific for either the human BACE1 gene or the human GAPDH gene. No significant differences in the levels of expression of BACE1 or GAPDH mRNA were observed among the cell lines.

(a 624-bp PCR product) and GAPDH mRNA (a 251-bp PCR product), a house keeping gene, were identified in these cell lines by RT-PCR analysis. The levels of BACE1 mRNA were comparable among these cell lines, whereas the levels of GAPDH mRNA were almost constant among them (Fig. 2D). Quantitative analysis, using GAPDH as an internal standard, showed that the levels of BACE1 mRNA expression were not statistically different among these cell lines (data not shown). These results indicate that the difference in BACE1 protein levels is not caused by a transcriptional regulation.

The above results suggest that wt PS1 significantly upregulates BACE1 maturation, presumably via facilitating the conversion of proBACE1 into mature BACE1 or stabilizing proBACE1. Conversely, PS deficiency and dominant–negative PS1 strongly downregulate it, indicating a novel role of PS1 for regulating BACE1 maturation.

Effect of γ-Secretase Inhibitors on BACE1 Maturation in Mouse Primary Neurons

To test whether PS1/γ-secretase activity directly affects the trafficking and maturation of BACE1 or not, we used two well-characterized γ-secretase inhibitors, L-685,458 and DAPT. Mouse primary neurons were treated with either 2 μM L-685,458, 1 μM DAPT or vehicle (DMSO) for 4 days. Equal amount of each cell lysate was subjected to Western blotting analysis using anri-BACE1 antibody (EE-17), anti-proBACE1 antibody, and anti-APP antibody (against the C terminus). As shown in Figure 3, we observed

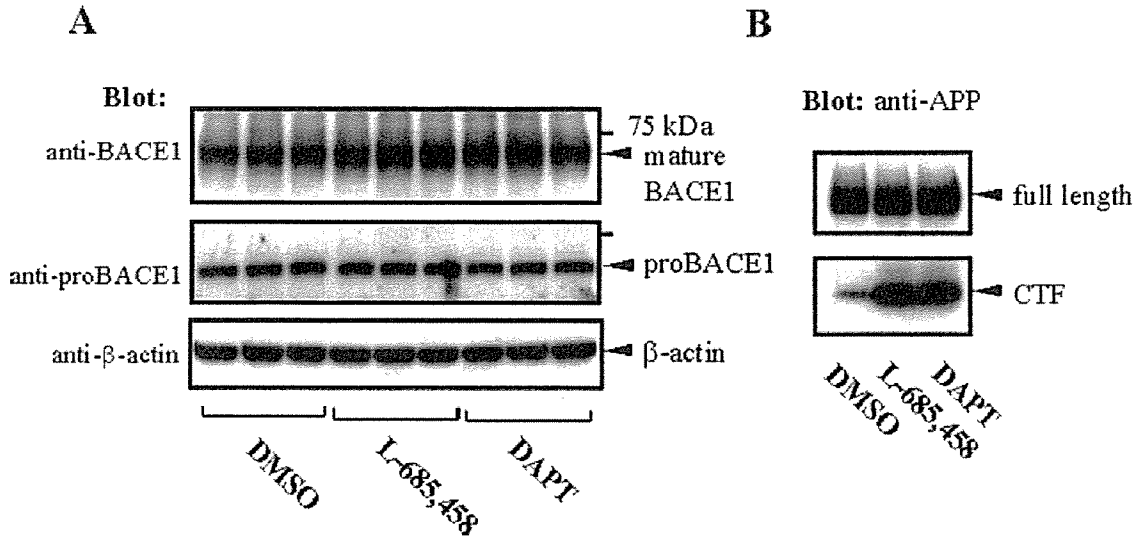

Fig. 3. Mouse primary neurons were treated with either 2 μM L-685,458, 1 μM DAPT or vehicle (DMSO) for 4 days. Equal amount of each cell lysate was subjected to Western blotting analysis using the indicated antibodies. No significant difference was seen in the levels of mature and proBACE1 between each treatment group (**A**), whereas APP CTF remarkably accumulated after each γ-secretase inhibitor, indicating that γ-secretase activity was effectively inhibited (**B**). One representative immunoblot is shown.

no significant difference in the levels of mature and pro-BACE1 between each treatment group (left panel), whereas APP C-terminal fragment remarkably accumulated after L-685,458 or DAPT treatment, indicating that γ-secretase activity was effectively inhibited (right panel). Thus, we consider that PS1/γ-secretase activity itself is less likely to be involved in the maturation process of BACE1.

PS1 and BACE1 Immunoprecipitation in the Cell and the Brain Tissue

A recent report showed that PS1 directly interacts with BACE1 in double transfected human embryonic kidney 293T cells (Hebert et al., 2003). We investigated whether wt PS1 and/or D385A PS1 can be associated with BACE1 in our experimental system. To answer this question, HA-tagged BACE1 and either wt PS1 or D385A PS1 were transiently co-expressed in PS−/− MEFs. The cells were harvested about 24 hr after transfection, and equal amounts of each cell lysate was immunoprecipitated using the anti-PS1 antibody against the N terminus, followed by the Western blot analysis using monoclonal anti-HA antibody. As shown in Figure 4A, wt (lane 1) and D385A PS1 (lane 2) were apparently associated with proBACE1 but not mature BACE1 in the transfected cells.

Next, we extended our findings obtained from the analysis of MEF cells to the SH-SY5Y cell lines. Equal amounts of cell lysate obtained from each cell line were immunoprecipitated using the anti-BACE1 antibody (targeting amino acids 487–501; Calbiochem). The cell lysates (Lys) as well as the immunoprecipitates (IP) were then subjected to Western blotting using the MAB5232 antibody (against the loop domain of PS1). As shown in Figure 4B, more PS1 C-terminal fragment (CTF) immunoreactivity was observed in wt PS1 cells (lane 7) than in control cells (lane 6), whereas almost no PS1 CTF bound to BACE1 was detected in D385A PS1 cells (lane 8; lower panel), reflecting the diminished endoproteolysis of D385A PS1 (lane 3). Conversely, solid association between the full-length D385A PS1 and BACE1 was observed (Fig. 4B, lane 8; upper panel). Furthermore, we showed the in vivo interaction between PS1 CTF and BACE1, using adult mouse brain tissue (Fig. 4C). The above results indicate that PS1 is preferably bound to proBACE1 rather than mature BACE1 and the functional binding can be contributed to the maturation of BACE1.

PS1 and BACE1 Colocalization in the SH-SY5Y Cells and Primary Neurons

To support the interaction between PS1 and BACE1 obtained from the immunoprecipitation experiment, we examined the intracellular localization of these two biochemical partners by immunofluorescent confocal microscopy, using control, wt PS1, and D385A PS1 SH-SY5Y cells. After permeabilization, cells were doubly stained with the antibody MAB5308 to visualize BACE1 and the anti-PS1 antibody (against the N terminus) to visualize PS1. As shown in Figure 5A–C, the PS1 in each cell line largely colocalized with the endogenous BACE1. Consistent with the above result shown in Figure 2A, an increase in wt PS1 immunoreactivity was apparently accompanied by an increase in endogenous BACE1 immunoreactivity (Fig. 5B, compared to 5A).

To further confirm the colocalization of PS1 and BACE1 in physiologically relevant system, endogenous PS1 and BACE1 were doubly immunostained in rat primary cultured cortical neurons at 5 days in vitro, using

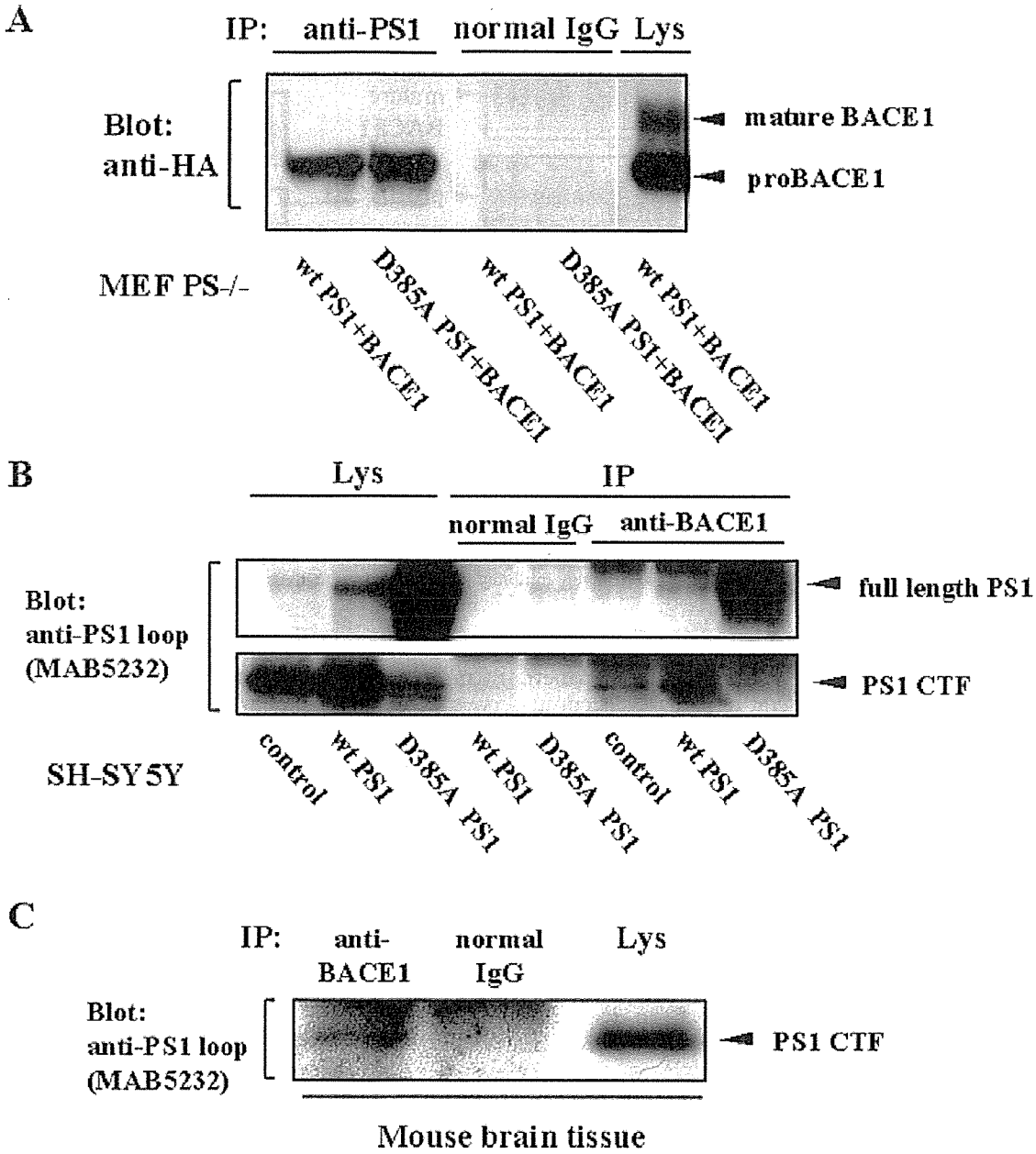

Fig. 4. PS1 and BACE1 physically interact with each other. **A:** HA-tagged BACE1 and either wt PS1 or D385A PS1 were transiently cotransfected into PS−/− MEFs. Each cell lysate was immunoprecipitated with anti-PS1 antibody against the N terminus. The cell lysate (Lys) as well as the immunoprecipitates (IP) were subjected to Western blotting with anti-HA antibody. ProBACE1, but not mature BACE1, was co-immunoprecipitated with either wt PS1 or D385A PS1. Almost no BACE1 immunoreactivity was observed from the samples of normal rabbit IgG used as negative controls. **B:** Equal amounts of cell lysates obtained from each SH-SY5Y cell line were immunoprecipitated using the anti-BACE1 antibody against the C terminus (Calbiochem), followed by Western blotting with the MAB5232 antibody against the loop domain of PS1. More PS1 C-terminal fragment (CTF) immunoreactivity was detected in wt PS1 cells (lane 4) than in control cells (lane 5). In D385A PS1 cells, almost no PS1 CTF bound to BACE1 was observed (lane 8: lower panel), reflecting the diminished endoproteolysis of D385A PS1 (lane 3). Conversely, solid association between full-length D385A PS1 and BACE1 was observed (lane 8: upper panel). Note that full-length wt PS1 was also associated with BACE1 in wt PS1 cells (lane 8: upper panel). No PS1 immunoreactivity was observed from the samples of normal rabbit IgG used as negative controls (lanes 5,6). **C:** Equal amounts of cell lysates obtained from adult mouse brain tissue were immunoprecipitated using the anti-BACE1 antibody (Calbiochem), followed by Western blotting using the MAB5232 antibody against the loop domain of PS1. PS1 CTF immunoreactivity was detected in the immunoprecipitates with the anti-BACE1 antibody (Calbiochem), whereas no PS1 CTF immunoreactivity was observed in the samples with normal rabbit IgG.